Forschungszentrum Karlsruhe

Technik und Umwelt

Wissenschaftliche Berichte

FZKA 6488

Sorption and Migration of Radionuclides in Granite (HRL ÄSPÖ, Sweden)

P. Vejmelka, Th. Fanghaenel, B. Kienzler, E. Korthaus, J. Roemer, W. Schuessler, R. Artinger

Institut für Nukleare Entsorgung

Forschungszentrum Karlsruhe GmbH, Karlsruhe

2000

The work was performed within the Project Agreement for collaboration on certain experiments related to the disposal of radioactive waste in the Hard Rock Laboratory Äspö (HRL) between the Bundesministerium für Bildung, Wissenschaft und Technologie (BMBF) and Svensk Kärnbränslehantering AB (SKB).

The authors thank the staff of HRL for preparation of rock and water samples and for the excellent cooperation.

Sorption and Migration of Radionuclides in Granite (HRL ÄSPÖ, Sweden)

Abstract

Within the scope of a bilateral cooperation an **Actinide Migration Experiment** is planned by INE to be performed at the Äspö Hard Rock Laboratory in Sweden. The experiment will be performed using fractured rock samples. The experimental set-up is constructed in order to fit into the CHEMLAB probe which allows to study the behavior of radionuclides under the most realistic conditions attainable. In preparation of these experiments, and to design the experimental setup, some sorption experiments (batch experiments and column experiments) with fracture filling material and granite, respectively, and with groundwater from the area of CHEMLAB were conducted under inert gas conditions (argon/1% CO_2) in the laboratory. In this paper the results of sorption experiments using actinides such as Pu, Np, Am are presented for both types of experiments. Details of the experimental setup are documented.

Geochemical model calculations for determination of the actinide tracer concentrations of the solution applied in the migration experiment are presented. In order to evaluate actinide breakthrough and recovery, the hydraulic properties of fractured rock samples are investigated. HTO is used as inert tracer at different flow rates. The results of the HTO experiments are modelled by means of matrix diffusion models.

Sorption und Migration von Radionukliden im Granit (HRL ÄSPÖ, Schweden)

Zusammenfassung

Im Rahmen einer bilateralen Zusammenarbeit ist von INE die Durchführung des **Actiniden Migration Experiments** im Hard Rock Laboratory ÄSPÖ in Schweden vorgesehen. Für das Experiment werden geklüftete Granitproben verwendet. Die Proben werden entsprechend den experimentellen Randbedingungen vorbereitet, so dass sie in die in ÄSPÖ verfügbare CHEMLAB Experimentiersonde eingesetzt werden können. Die in situ Experimente ermöglichen das Studium des Verhaltens der Radionuklide unter den weitestgehend natürlichen phyikalisch/chemischen Bedingungen. Zur Vorbereitung der in situ Experimente und zur Auslegung der experimentellen Randbedingungen wurden zunächst Sorptionsexperimente (batch- und Säulenversuche) mit Kluftfüllmaterial und Granit unter Verwendung von Grundwasser aus der Umgebung des CHEMLAB unter Sauerstoffausschluss (Ar/1%CO2) im Labor durchgeführt. Im vorliegenden Bericht wird über die Ergebnisse der Sorptionsexperimente berichtet, die mit den Radionukliden Pu, Np und Am durchgeführt wurden. Einzelheiten der experimentellen Anordnung werden beschrieben.

Zur Vorhersage der Actinidenkonzentrationen unter den in situ Bedingungen wurden geochemische Modellrechnungen durchgeführt. Um die Actinidenmigration und das Recovery ermitteln zu können, wurden die hydraulischen Eigenschaften der klüftigen Granitproben bestimmt. HTO wurde als inerter Tracer bei unterschiedlichen Fließgeschwindigkeiten verwendet. Die Ergebnisse der HTO-Experimente wurden unter Anwendung eines Matrix-Diffusions-Modells modelliert.

Contents

List of figures

List of Tables

1 Introduction

The Äspö Hard Rock Laboratory (HRL) was established in Sweden in a granite rock formation for in-situ experiments with radionuclides (Jansson 1997). The aims of this facility are:

- To examine which methods are most suitable for research in the bedrock.
- To develop and demonstrate methods for deciding in what way a deep repository can be planned and constructed in accordance with the local characteristics of the bedrock.
- To increase scientific understanding of a deep repository's safety margins.
- To develop and demonstrate the technique that will be used during the disposal of spent nuclear fuel.

One tool which is available at Äspö HRL is a drill hole probe CHEMLAB which can be used to investigate actinide elements under the pressure and geochemical conditions of the host rock. The experiments planned by INE to be performed with the CHEMLAB are to study the behavior of radionuclides with respect to diffusion, migration, solubility, and sorption under the most realistic conditions attainable. Within the scope of a bilateral co-operation, INE plans migration experiments with actinides such as Pu, Am, and Np.

The objectives of the experiments are:

- investigation of applicability of radionuclide retention coefficients measured in batch experiments for in-situ conditions
- to validate the radionuclide retardation measured in laboratories by data from in-situ experiments in rock
- to demonstrate that the laboratory data are reliable and correct under the conditions prevailing in the rock
- to reduce the uncertainity in the retardation properties of the radionuclides americium, neptunium and plutonium.

In preparation of these experiments, and to design the experimental setup, some first orientating sorption experiments (batch experiments and column experiments) with fracture filling material and granite, respectively, and with groundwater from the area of CHEMLAB were conducted under inert gas conditions (argon/1% CO_2) in the laboratory. Figure 1 shows a schematic representation of the CHEMLAB design.

As a prerequisite of the CHEMLAB experiments a series of laboratory experiments have to be performed at INE. These investigations cover

- Characteristics of groundwater and rock material (granite and altered fracture filling material)
- Sorption behaviour of actinides onto solid phases
- Characterisation of the fractures with respect to groundwater flow
- Development and test of the experimental setup for the CHEMLAB probe
- Determination of the breakthrough and recovery of the actinides in order to design the experimental schedule and analytical requirements

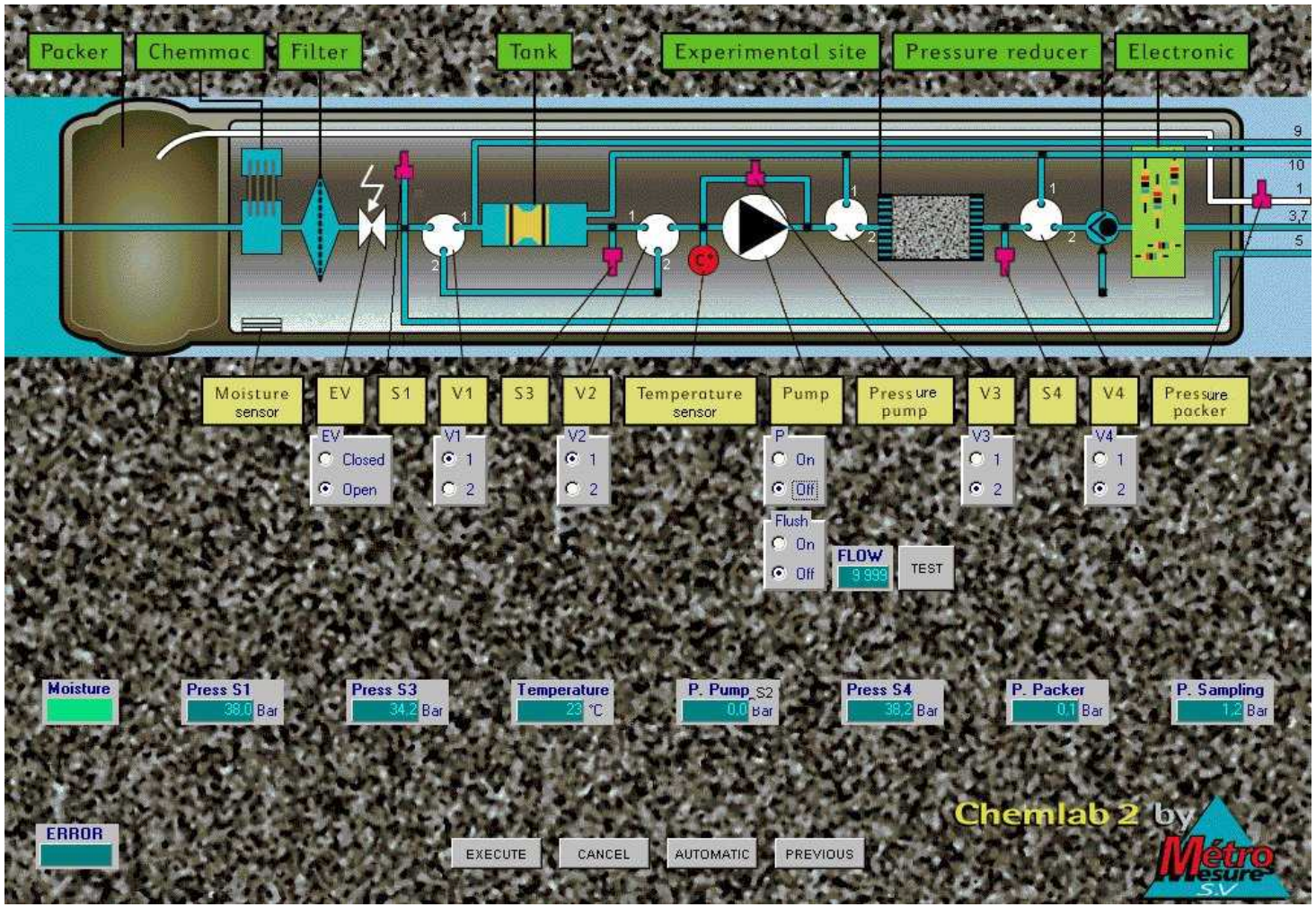

Fig. 1 Scheme of the “CHEMLAB” – System, used for **Actinide Migration Experiment** in the Hard Rock Laboratory “ÄSPÖ”

2 Laboratory Experiments

2.1 Characterization of the Starting Materials

2.1.1 Characterization of the ÄSPÖ Groundwater

Groundwater was extracted from the SA 2600 level in connection with the production of drill cores for the migration experiments. The groundwater (150 l) was extracted under anaerobic conditions. The physico-chemical parameters of the groundwater as measured in situ are these:

Temperature	12.8°C
Oxygen concentration	0.1 mg/l
Redox potential (after 2 h)	112 mV (with decreasing tendency)
pH	7.5
Conductivity	4.0 mS/cm
Acid capacity (Ks) up to pH 4.3	2.15 mmol (eq)/l

The contents of cations and anions as well as the carbon content were determined in the laboratory. The findings are summarized in Tab I.

Tab I Composition of the ÄSPÖ groundwater (mg/l)

	Cations										
	Zn	Si	Mn	Fe	Mg	Ca	Al	Sr	Li	Na	K
Unfiltered	0.23	5.48	0.57	0	69.17	1588.8	1.66	25.2	1.10	2149.8	11.65
450 nm	0.22	5.39	0.60	0	73.19	1552.0	1.65	25.7	1.05	2253.2	10.64

	Anions						
	F^-	Cl^-	NO_3^-	PO_4^{3-}	SO_4^{2-}	IC	TOC
Unfiltered	0.1	7045.2	0.1	0.1	308.5	19.92	3.78
450 nm	0.1	6963.1	0.1	0.1	308.5	19.76	4.08

2.1.2 Characterization of the Fracture Filling Material

Fracture filling material was extracted from open fractures at various places in the HRL during a visit of INE staff at ÄSPÖ. The samples were extracted under aerobic conditions, and the fracture filling material had been in contact with air since the underground laboratory had been constructed.

In the laboratory, the elemental composition of the samples was determined by RFA, and the mineralogical constituents were determined by X-ray diffraction analysis. The results of the RFA examinations are listed in Tab II. Fig. 2 shows a typical X-ray diffraction diagram.

Tab II Elemental composition of various ÄSPÖ fracture filling materials (wt. %)

	Sample name							
	A	B	2220	2250	2260	29603	29603 ≤ 1 mm	29603 ≥ 1 mm
MgO	0.32	0.40	1.90	1.94	2.30	0.69	0.61	0.73
Al_2O_3	11.99	15.04	17.81	13.71	14.19	14.30	17.00	14.30
SiO_2	70.65	70.86	58.40	60.9	57.88	66.79	65.03	65.23
SO_3	0.23	0.09	0.06	0.17	0.09	0.03	0.01	0.02
CaO	1.63	1.36	4.43	4.23	4.62	2.34	2.37	2.57
TiO_2	0.32	0.35	0.76	0.84	0.92	0.41	0.39	0.43
Fe_2O_3	2.04	2.15	5.56	5.87	6.57	3.07	2.81	3.07
Na_2O	1.49	1.91	2.53	2.45	2.35	2.92	2.64	2.27
K_2O	5.62	5.75	2.98	2.77	2.81	3.87	4.08	4.37
SrO	0.035	0.027	0.120	0.107	0.126	0.074	0.085	0.078
ZnO	0.003	0.004	0.011	0.013	0.013	0.007	0.006	0.007
P_2O_5	0.083	0.089	0.399	0.422	0.452	0.173	0.155	0.167
MnO_2	0.044	0.057	0.105	0.106	0.123	0.064	0.061	0.068
ZrO_2	0.034	0.035	0.046	0.048	0.050	0.038	0.032	0.033
BaO	0.088	0.094	0.164	0.152	0.156	0.131	0.150	0.150
Total amount	94.59	98.21	95.29	93.83	92.66	95.91	95.42	93.50

The main constituent in all samples found to be SiO_2 with a share of 60 to 70 wt.%. Al amount to 12 and up to a maximum of 18 wt.%. Sample No. 29603 was chosen for the batch tests because it was the only sample of which a sufficient amount of material was available. This sample was analyzed once in its original state and then separated into fractions, one >1 mm and one <1 mm. Results show that both fractions are of comparable composition.

The X-ray diffraction diagrams are comparable for all samples. The main phase is quartz, and microcline, albite and sepolite have been detected in addition.

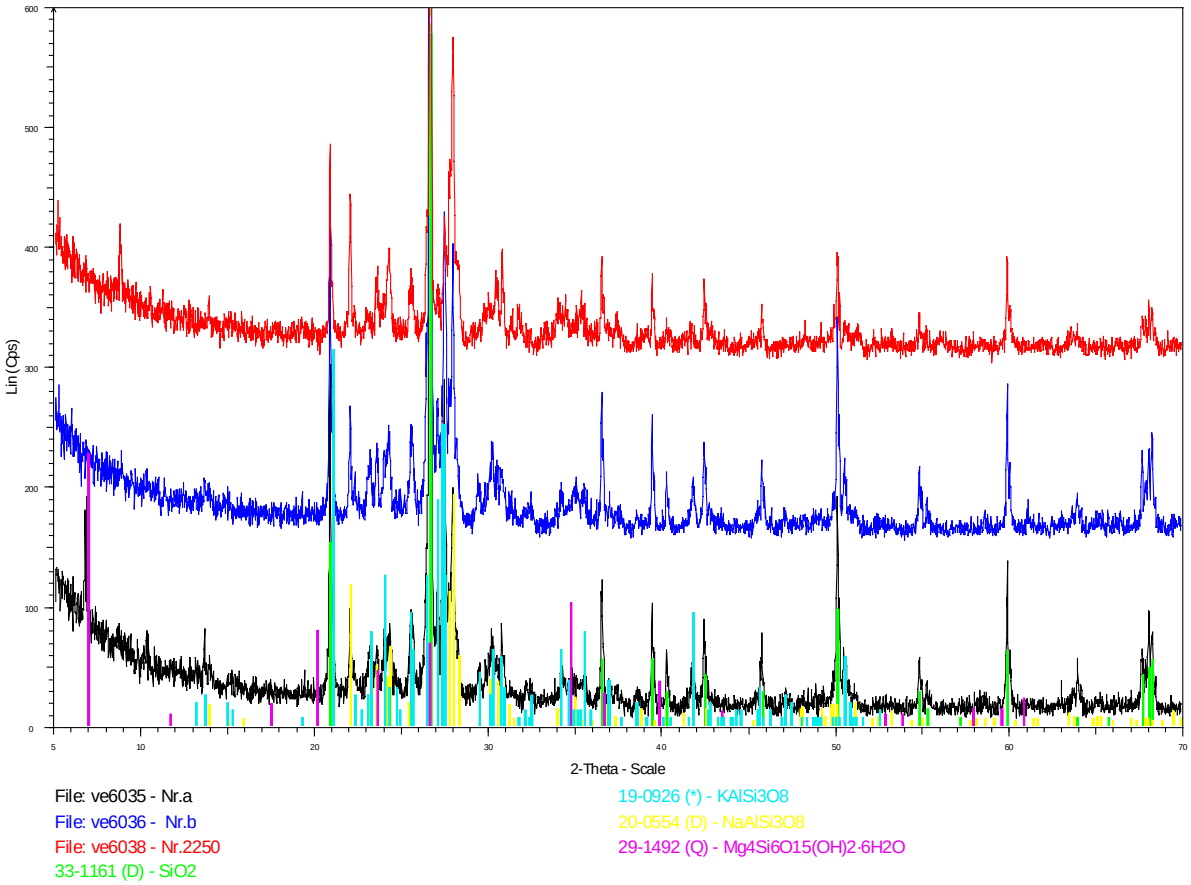

Fig. 2 X-ray diffraction pattern of the ÄSPÖ-fracture filling material

2.2 Batch Experiments

Batch experiments with fracture filling material and granite were conducted to obtain information about the sorption behavior of Pu, Am, and Np. Fig. 3 gives a schematic diagram explaining the sorption experiments. First, groundwater is contacted with the solid under investigation, then it is separated from the precipitate (filtration over 450 nm), and doped with a radionuclide stock solution I. The resultant radionuclide stock solution II is again contacted with the conditioned solid after an equilibrium has been established.

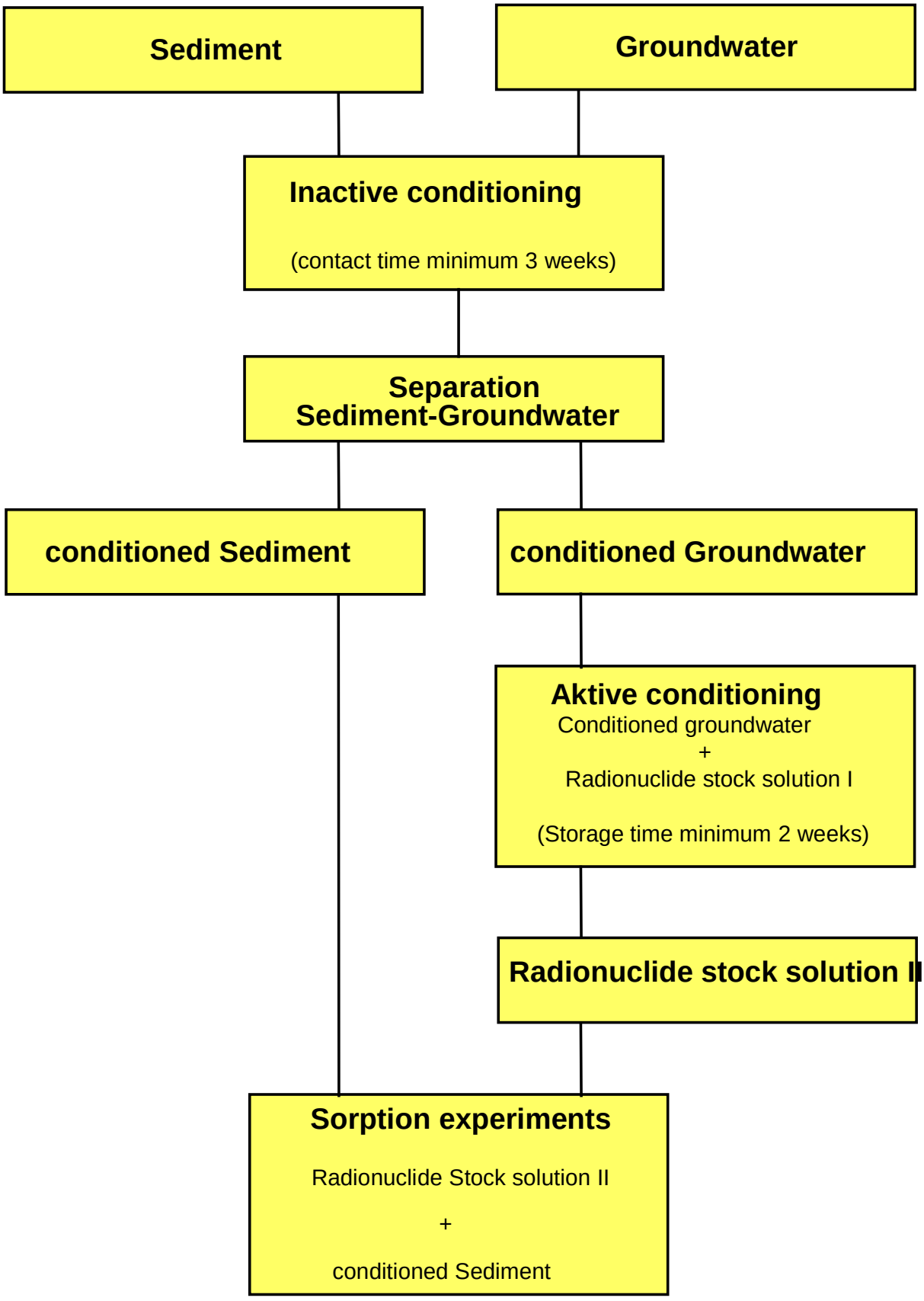

Fig. 3 Schematic outline of the batch sorption experiments.

The following parameter sets were selected for the experiments:

- Unconditioned groundwater was treated with solutions of the radionuclides and added unconditioned fracture filling material.

- Groundwater was conditioned with the two fractions of sample No. 29603, separated, and treated with the radionuclide solution. Subsequently, these groundwater samples were treated with the conditioned fracture filling material.

- Granite was conditioned with groundwater, and the conditioned groundwater was treated with a radionuclide solution.

Separate stock solutions II and sorption samples were prepared for the different radionuclides. For all experiments, a v/m ratio of 4 ml/g was selected; the experiments were run under anaerobic conditions (Ar/1% CO_2 atmosphere).

Radionuclide Stock Solutions I:

The stock solutions I used to dope the groundwater samples were composed as follows:

Pu-238	~ 1 E-4 mol/l, in 0.05 m HCl
Am-241	~ 1 E-4 mol/l, in 0.1 m HNO_3
Np-237	~ 1 E-2 mol/l, in 1 E-4 m HCl

Radionuclide Stock Solutions II:
The radionuclide concentrations of the resultant stock solutions II (conditioned groundwater doped with stock solution I), at the beginning of the sorption experiments, were for

Pu-238:	~ 5 E-9 mol/l
Am-241	~ 5 E-9 mol/l
Np-237	~ 1 E-5 mol/l.

2.2.1 Results of the Sorption Experiments

2.2.1.1 “Groundwater + fracture filling material” unconditioned System

Figure 4 shows the dependence on time of the radionuclide concentration for stock solutions II and for the sorption samples. The numerical values of the radionuclide concentrations are listed in Tab V in the Annex. Even after a few days of contact, sorption is observed for Pu and Am and, after 57 days, the radionuclide concentrations have nearly reached the limit of detection.

Traceable sorption is observed for Np only after some 15-20 days. Afterwards, however, the Np concentration in the sorption samples decreases to the limit of detection while, in the stock solution, it remains constant over the entire test period. The decrease of the Np concentration in the sorption samples is attributed to the reduction of Np (V) to Np (IV) (Lieser 1991). Either Np (IV) is sorbed much more strongly than Np (V) and/or it is precipitated as sparingly soluble Np (IV) hydroxide.

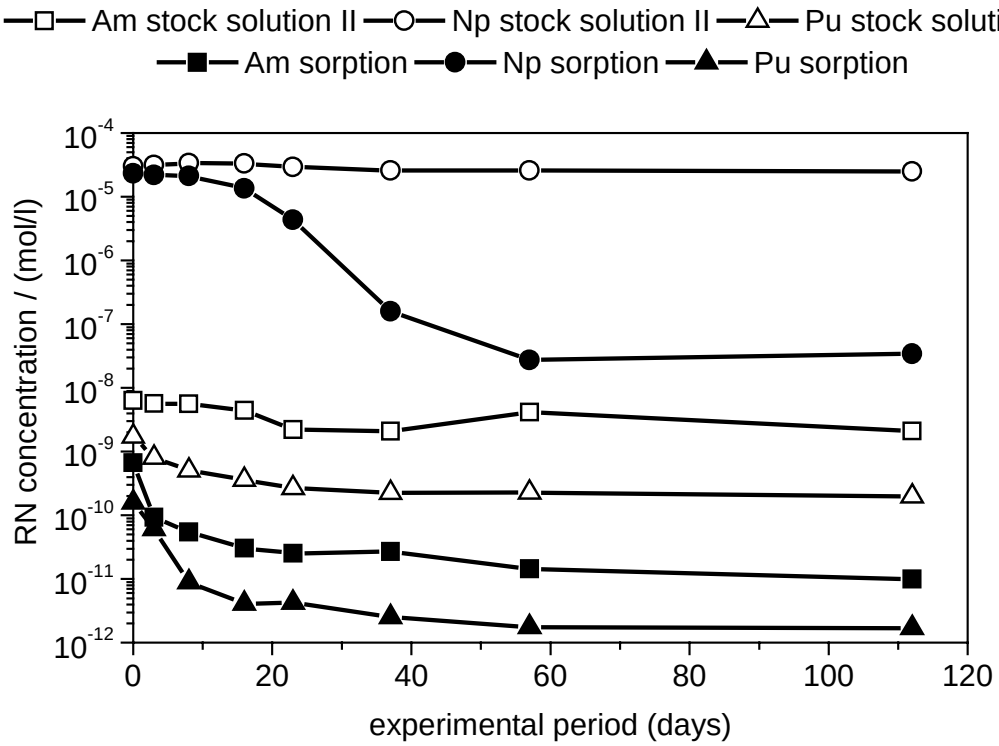

Fig. 4 Development, as a function of time, of the RN concentrations in the sorption samples of the “unconditioned groundwater/fracture filling material” system.

The redox potential of the sorption samples is approx. 50 mV. The pH of the sorption samples amounts to 6.50 to 6.70. The reducing effect of the fracture filling material can be attributed to its Fe content (magnetite). After 115 days, sorption coefficients of 3360 ml/g are calculated from the radionuclide concentrations for Pu, 2800 ml/g for Am, and 3900 ml/g for Np.

2.2.1.2 “Groundwater + Fracture Filling Material” Conditioned System

A fraction of the fracture material ≤1 mm and a fraction ≥1 mm were used for the experiments. In this report, these two fractions will be referred to below simply as “fine” and “coarse,” respectively. The material was conditioned with groundwater for 7 days, then the groundwater was separated, and treated with the radionuclide stock solution I. The tracer-

labeled groundwater was again contacted with the preconditioned solid. Fig. 4 to Fig. 8 show the development, as a function of time, of the radionuclide concentrations in the stock solutions II and the sorption samples. The numerical values of the radionuclide concentrations are listed in Tab V to Tab IX in the Annex.

The results also exhibit relatively good agreement with the results obtained with the unconditioned system. The pH levels of the sorption samples are 6.50 to 6.70. The redox potential of the sorption samples with the <1 mm fracture filling material amounts to approx. 150 mV, while the potential for the >1 mm fraction samples is lower, amounting to -100 mV.

Plutonium

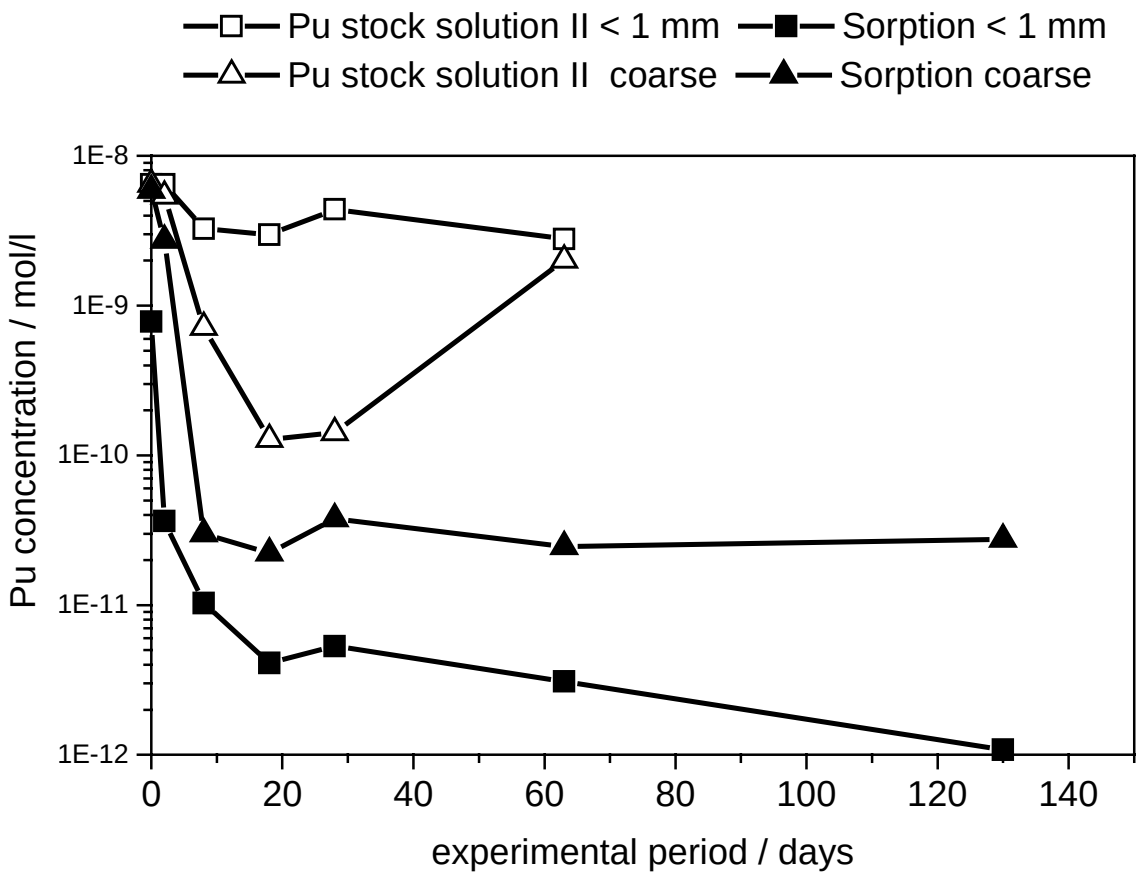

Fig. 5 Development, as a function of time, of the Pu concentration in the sorption samples of the "conditioned groundwater/fracture filling material" system.

For both fractions, evident sorption of Pu is observed relatively quickly. The sorption is slightly higher for the fine fraction than for the coarse fraction. For the samples of the fine fraction, the limit of detection of Pu is reached after approx. 60 days, while the Pu concentration in the samples with the coarse fraction remains more or less constant between 10 and

60 days and is clearly above the limit of detection. Further studies, e.g. by ultrafiltration, are planned to detect the cause of this difference.

Another striking fact is the different stability of Pu in the stock solutions II. In the stock solution II of the coarse fraction, the Pu concentration clearly decreases in the course of the experiment from 6.5 E-9 mol/l to 1.4 E-10 mol/l, and then rises again, while, in the stock solution II of the fine fraction, the Pu concentration is relatively constant in the range between 6.5 E-9 mol/l and 4.4 E-9 mol/l.

Americium

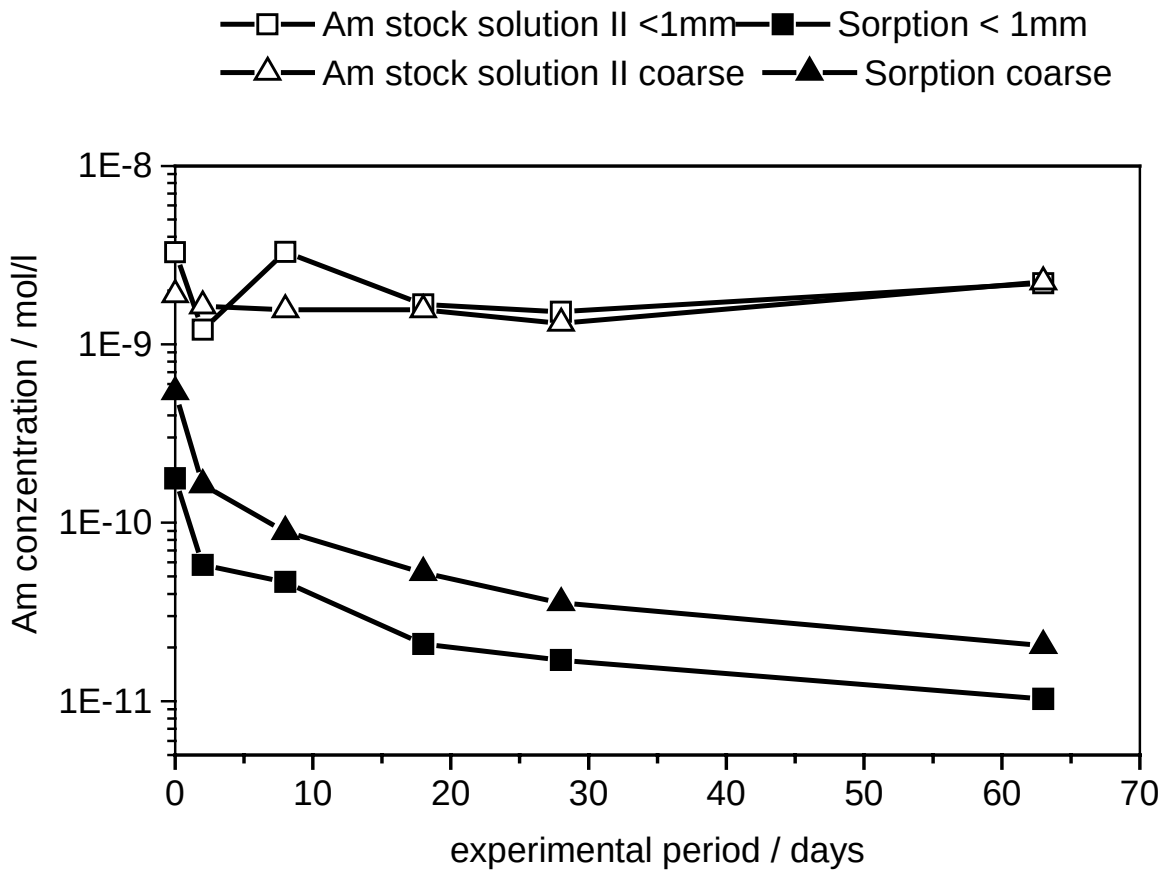

Fig. 6 Development, as a function of time, of the Am concentration in the sorption samples of the “conditioned groundwater/fracture filling material” system.

Also americium is sorbed relatively quickly and to a high extent in both fractions. As in the case of Pu, sorption is slightly higher in the fine fraction than in the coarse fraction. In the experimental period of 63 days so far, a steady increase in sorption has been observed. Consequently, it can be assumed that, as the experiment goes on, the limit of detection of

Am will be reached. In contrast to the situation with Pu, the Am concentrations are constant over the duration of the experiment in both stock solutions II.

Neptunium

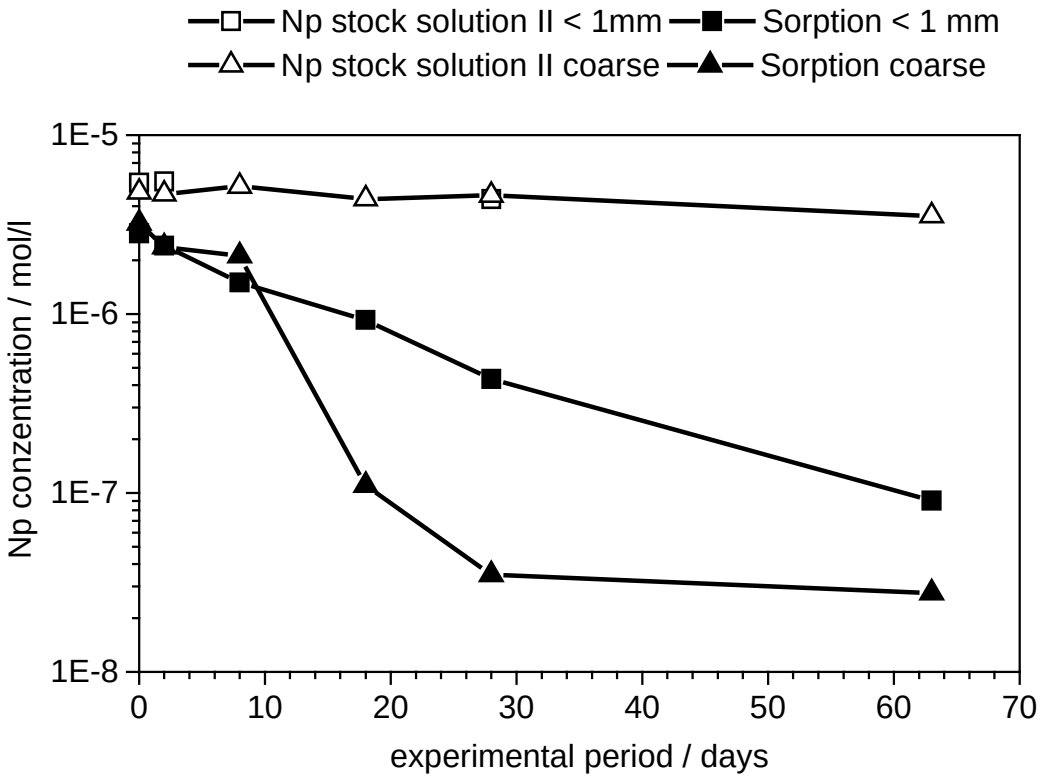

Fig. 7 Development, as a function of time, of the Np concentration in the sorption samples of the “conditioned groundwater/fracture filling material” system.

As in the case of Pu and Am, different degrees of sorption in the two fractions are observed for Np. In the fine fraction, sorption increases slowly but steadily. In the coarse fraction, a clear increase in Np sorption is observed after 10 days, which is comparable to the clear increase in the experiments with unconditioned fracture filling material, and the limit of detection for Np is reached after a test period of 63 days. This clear increase in sorption again can be made to correlate with the redox potential, which is approx. -100 mV for the sorption samples of the coarse fraction and thus is clearly more negative than the approx. 150 mV for the sorption samples of the fine fraction. In the test period so far, the Np concentration in the stock solution II has been relatively constant.

2.2.1.3 “Groundwater + Granite” Conditioned System

As the fractures and fissures containing the fracture filling material are surrounded by granite, also this material must be considered for radionuclide transport, as it is available for surface sorption. For this reason, batch experiments were conducted with granite and groundwater. As described above, the materials were first contacted for a couple of days before the beginning of the experiments. The pH levels of the sorption samples are 6.30 to 6.40, the redox potential is approx. 50 - 150 mV.

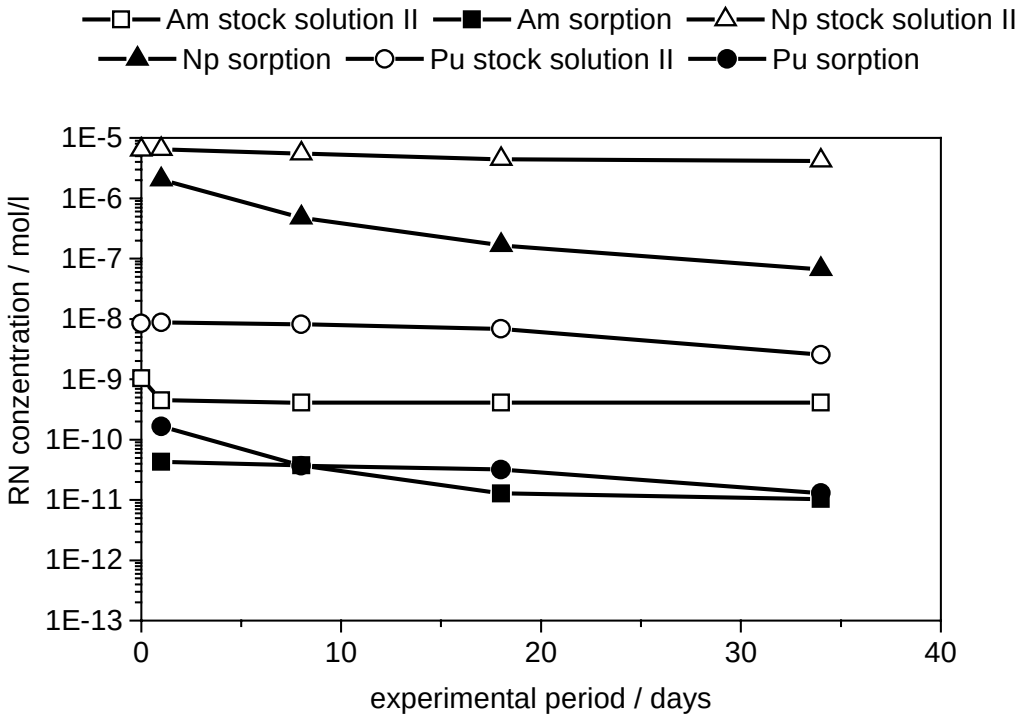

Fig. 8 Development, as a function of time, of the Rn concentration in the sorption samples of the “conditioned groundwater/ÄSPÖ granite” system.

The results are shown in Fig. 8. Evident sorption is observed for all radionuclides. Am and Pu show marked sorption already after a very brief contact period, while a slower, but steadier increase in sorption with contact time is observed for Np. Additional measurements over longer periods of the experiment have shown that, also under these conditions, the limit of detection of the radionuclides is achieved in the sorption samples. Again, the evident sorption of Np can be correlated with the redox potential of the sorption samples, which is 50 - 150 mV. At levels below 100 mV, Np (V) can be reduced to Np (IV), which has a lower solubility and higher sorption.

As in the fracture filling material, the reducing effect of granite can be attributed to its Fe content (Eliason 1993).

2.3 Column Experiments

2.3.1 Column Experiment with Fracture Filling Material

In a first preliminary experiment, the migration behavior of Np (V) was studied with in situ fracture filling material and groundwater. For this purpose, the fracture filling material with a grain size <1 mm was incorporated in a column 10 cm long and with an inner diameter of 1 cm (porosity 22.7 %), and conditioned with the SA 2600 A groundwater for two weeks.

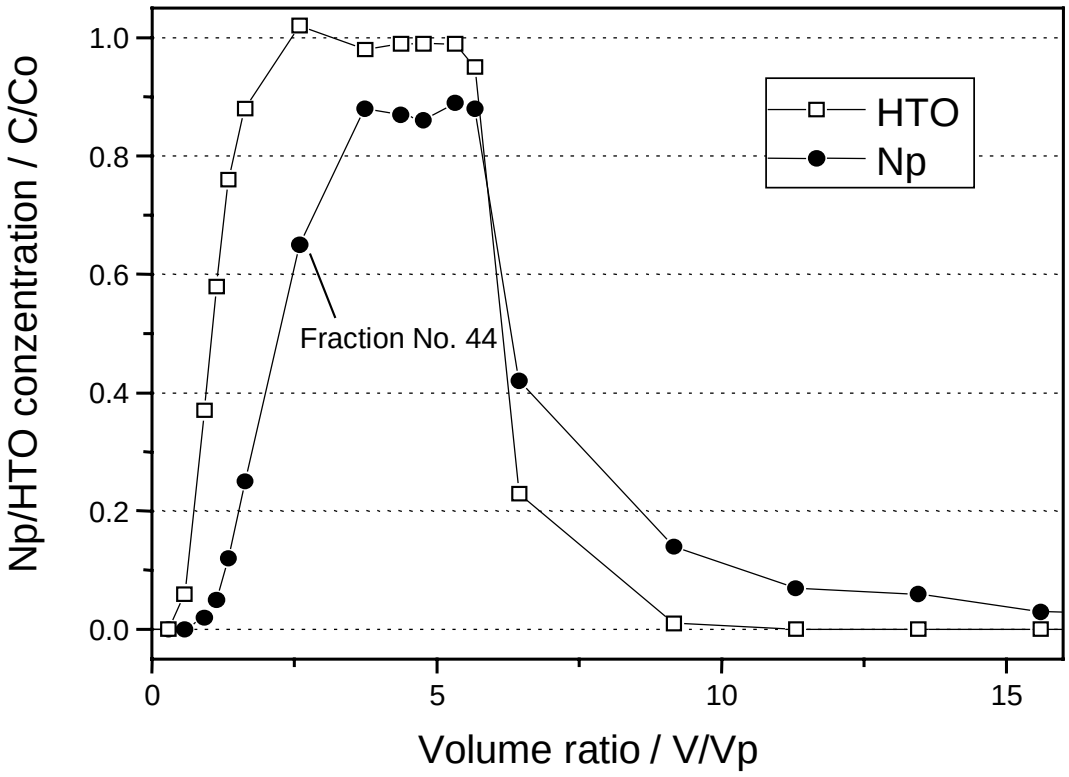

Fig. 9 Np and HTO breakthrough curve for the “fracture filling material/groundwater” ÄSPÖ system. (Np concentration added: 1.1 x 10^{-5} mol/l, pump rate: 0.69 m/d.)

The inert gas atmosphere provided consisted of Ar + 1 % CO_2. The resultant pH amounted to 7.0, and the redox potential was 200 to 300 mV. The nuclide used was Np-237 ($t_{1/2}$ = 2.14 x 10^6a) as Np (V), which was added with a permanent impulse of 5.2 pore volumes. The activity contribution by the Pa-233 daughter nuclide was determined by α/β discrimination.

Fig. 9 shows the breakthrough curves obtained for Np and HTO. As can be seen, Np is eluted slightly later than the tritiated water. This retardation, R_f, is approximately a factor of 2, i.e. Np is eluted with a delay of 1 pore volume compared to water. The recovery of Np is 95%.

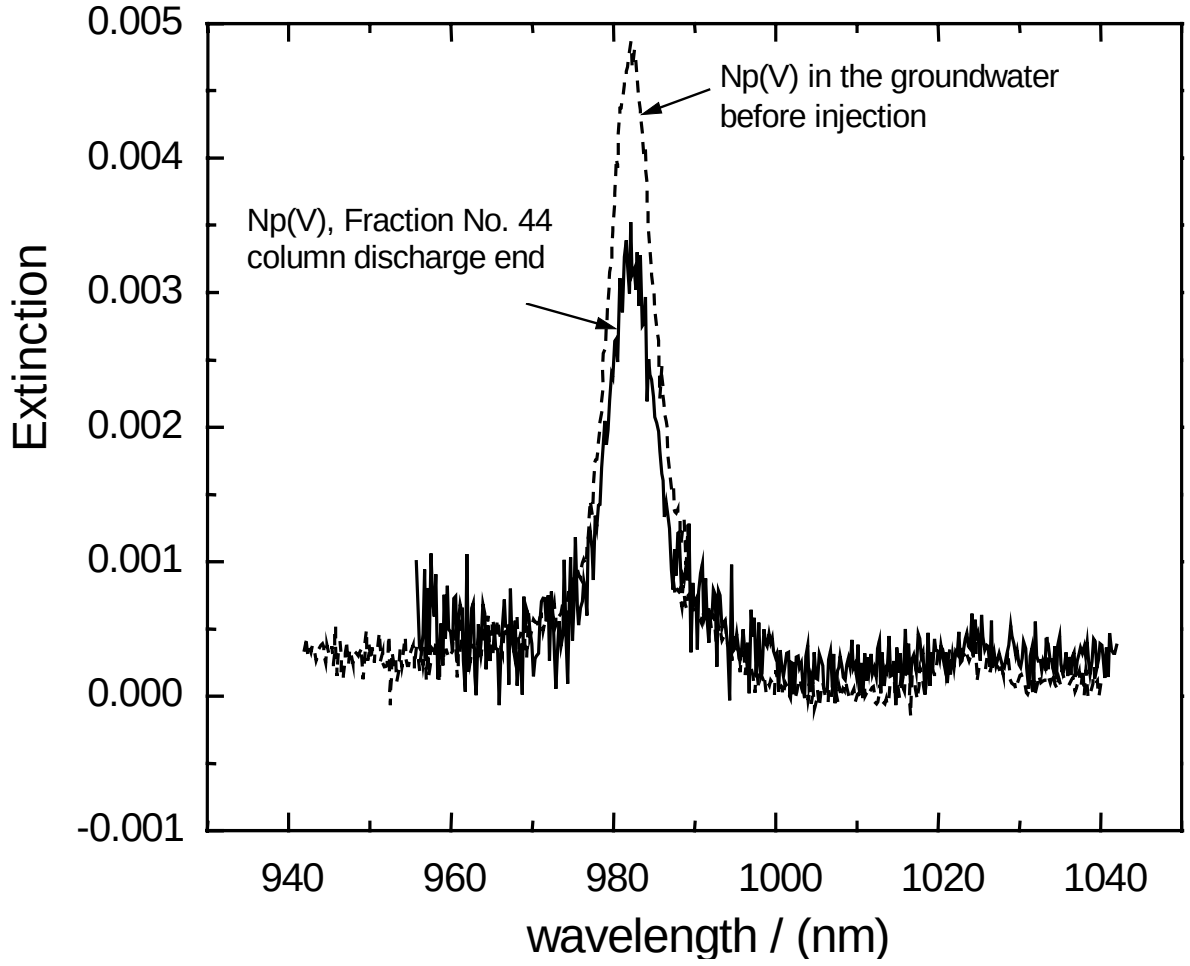

Fig. 10 Np absorption spectra of the injected solution and eluate fraction 44.

Spectroscopic evaluation of eluate fraction No. 44 in Fig. 10 shows the NpO_2^+ concentration to be 35% lower than in the starting solution. As the activity concentration is also 35% lower, and Np (V) is present in the starting solution, it may be concluded that Np migrates in its pentavalent oxidation level as an NpO_2^+ ion. The existence of an ionic Np species is confirmed by ultrafiltration of the starting solution and of the eluate. This allows colloid-borne Np transport to be excluded. That the migration of Np (V) is observed in the column experiments performed is due to the small dimensions of the column and, consequently, the short dwell time in the column of the migrating Np.

As the results of the batch experiments show, longer contact times are necessary for the reduction of Np (V) to Np (IV), for which a clearly higher degree of retention would be expected. However, for such column experiments, the column would have to be markedly larger, and also clearly more fracture filling material would be required than was available.

3 Characterization of Core Samples for Laboratory and In Situ Experiments

3.1 Preparation of the Core samples

To run the migration experiments in CHEMLAB, a core sample with a fracture must be placed into an autoclave and the hydraulic properties of the fracture must be known. For this purpose, experiments were conducted initially on the tight enclosure of core samples in an autoclave. The core sample chosen, with a continuous fracture, were placed in a sleeve of stainless steel, and the periphery was filled with epoxy resin. The top and the bottom ends were closed with acrylic glass covers sealed relative to the stainless steel sleeve with an O-ring, and which contained the bore for feeding and extracting the groundwater lines. Fig. 11 show the construction drawing of the autoclave and Fig. 12 to Fig. 14 show a core sample with the fracture, the core sample in the autoclave and the complete autoclave in a glove box.

The tightness of the column was tested in subsequent laboratory experiments in which the column was exposed to 60 bar of fluid pressure. The experiments indicate that the columns were leaktight up to the 60 bar of pressure applied. The fluid pressure in CHEMLAB is about 27 bar; consequently, no leakage of the columns is to be expected under in situ conditions. A total of three columns of the appropriate dimensions were prepared out of the core samples available and can now be used for the laboratory and in situ experiments.

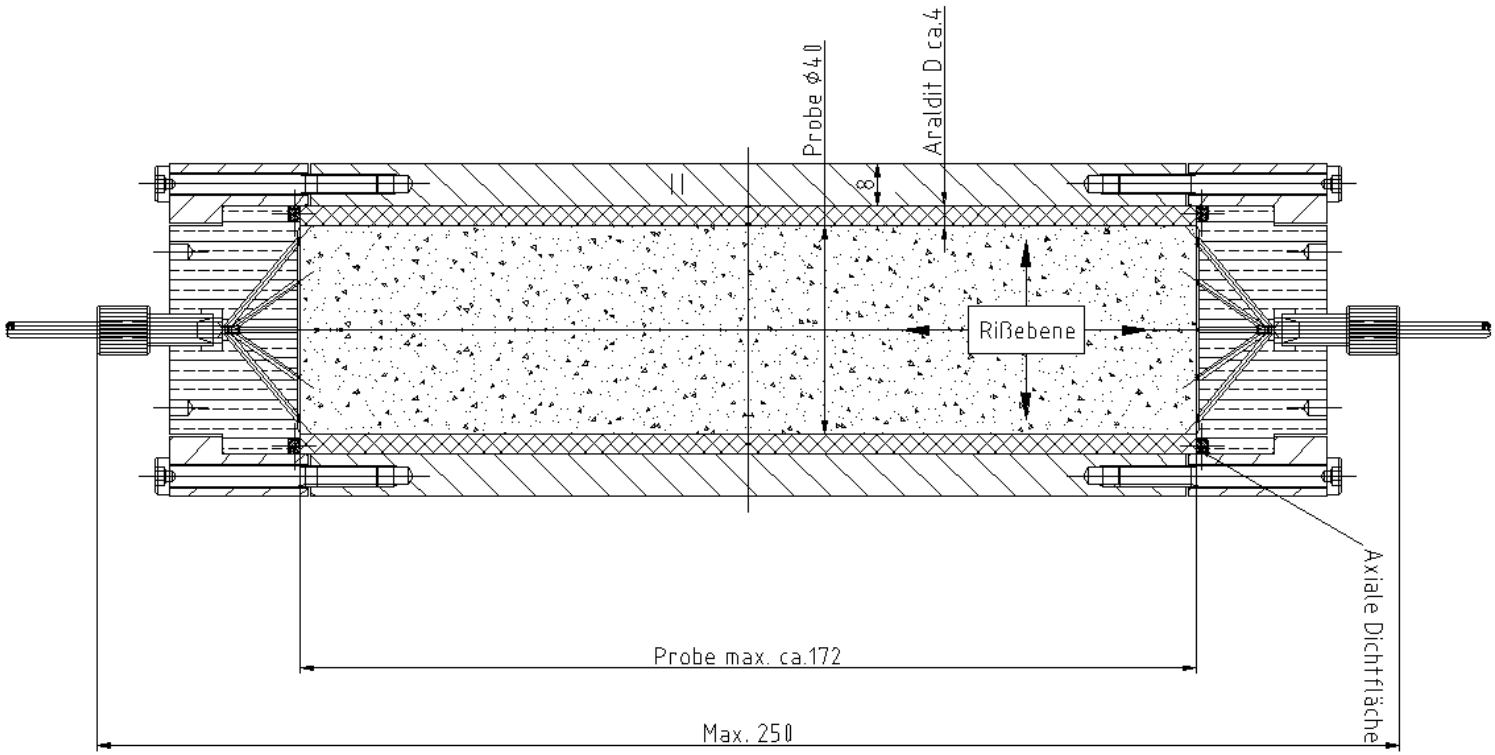

Fig. 11 Set-up of the experiment: Autoclave, fractured core, lid and draining system
The inner diameter of the autoclave was adjusted to the diameters of the cores.

Fig. 12 ÄSPÖ core sample with fracture.

Fig. 13 ÄSPÖ core sample embedded in a stainless steel sleeve; top and bottom ends.

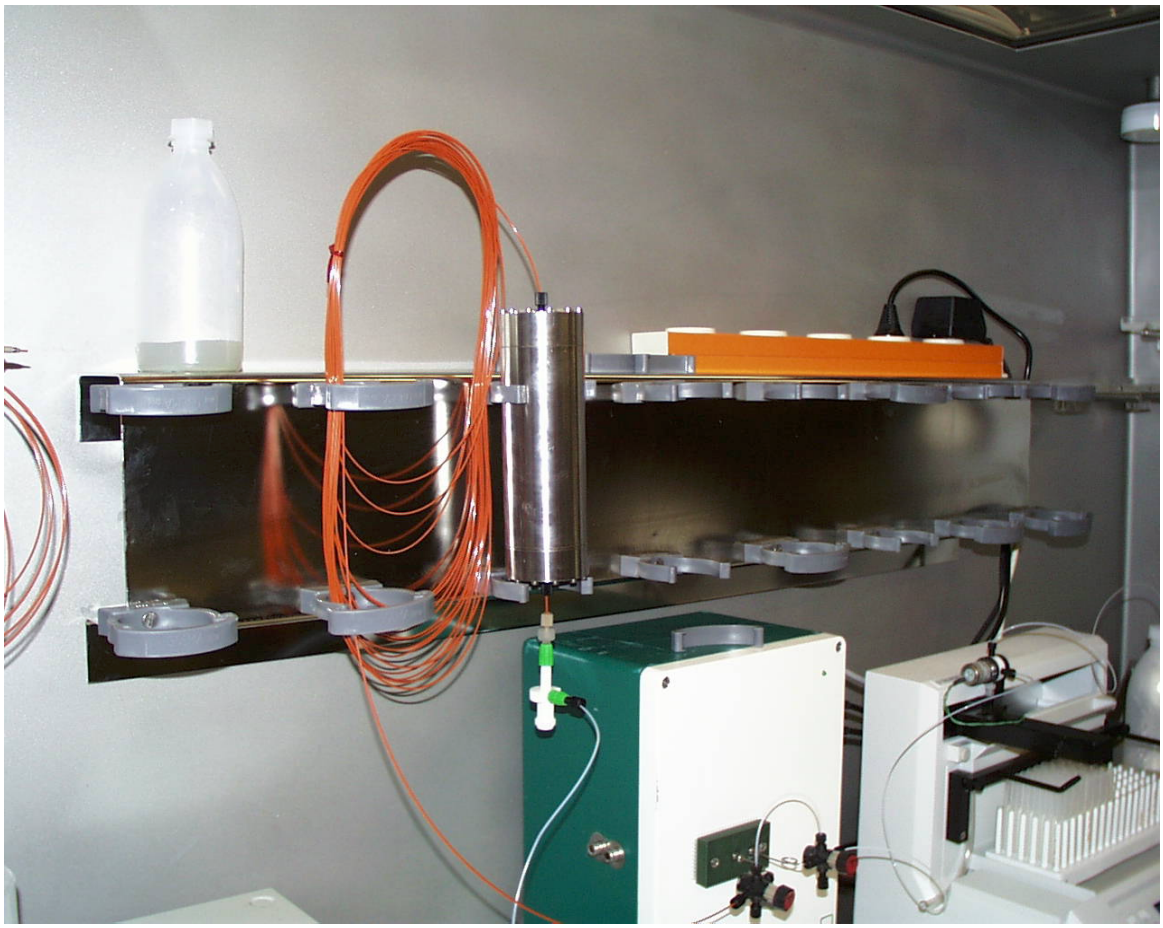

Fig. 14 Laboratory setup with the ÄSPÖ column for migration studies.

3.2 Analytical investigations of the solids in the fracture

A piece of Äspö rock drilling core was analysed by SEM in microscopic view (magnification 10x). The fracture in the rock can be seen as a green ribbon at the cylindrical surface of the drilling core. This part of the surface was grinned about 2 mm in depth and polished. Fig. 15 shows the SEM-back-scattered electron image of this part. The limits of the visible fracture is marked by white stars (*), because they are undetectable under this mode. The back-scattered electron mode shows differences of the elemental composition, only. Parts of the surface contain elements having higher periodic number are shown in lighter colors.

The four light spots indicate ironoxide containing particles with a Fe-concentration of a factor of 200 higher than in the surrounding rock. In Fig. 16 EDX-analysis (energie dispersive xray) of this particles is compared to the average rock.

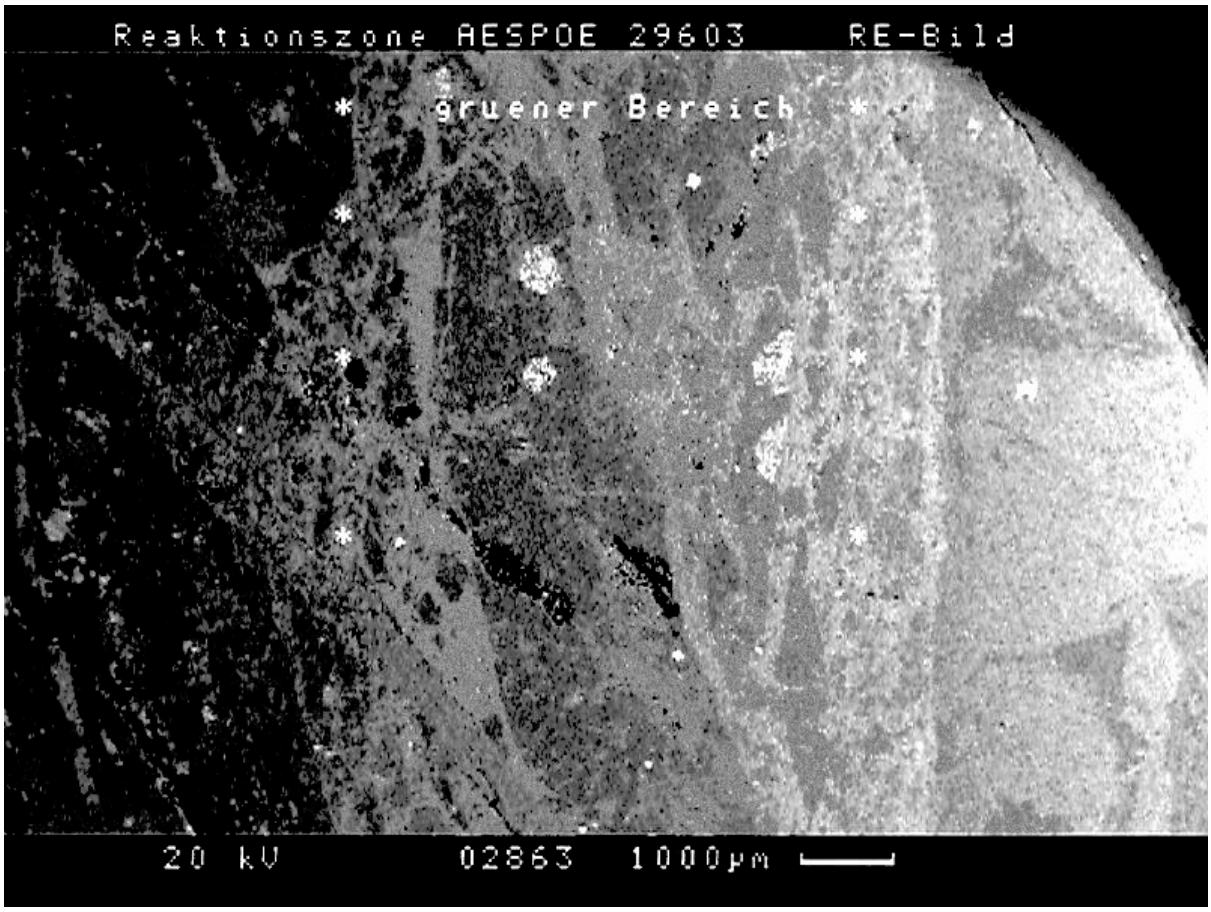

Fig. 15 SEM-image of a fracture

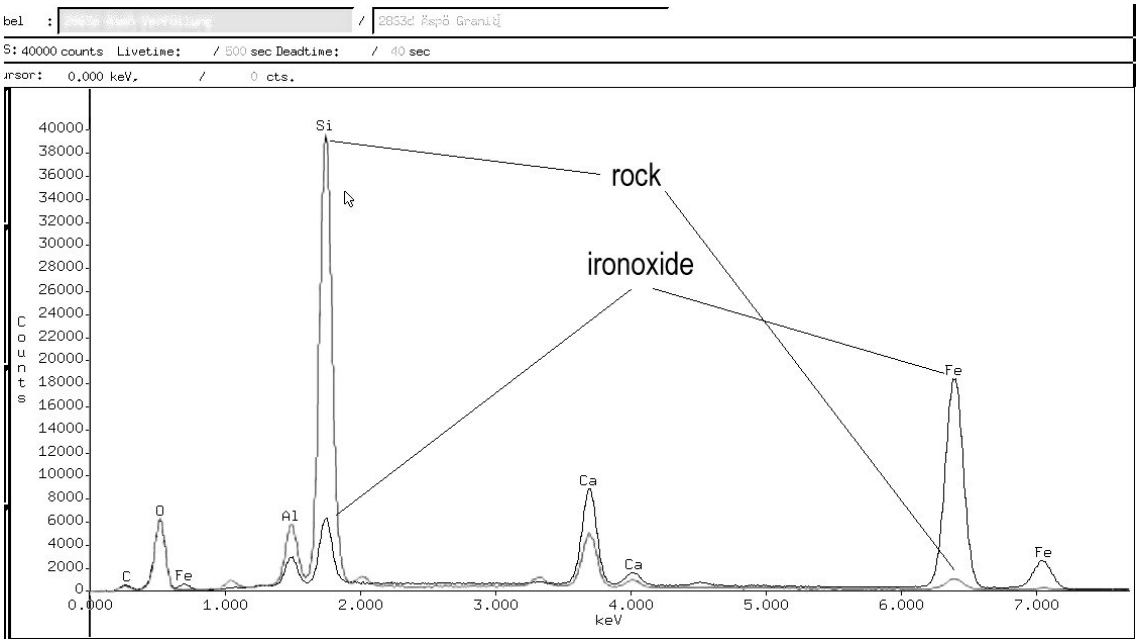

Fig. 16 EDX analysis of the average rock and an Fe-particle

For a better identification of the mineralogical phases, Fig. 17 shows an element mapping of this region. The iron-oxide particles dominate the Fe-mapping. The main part of the rock consists of silicon, aluminium, and potassium containing phases. The inclusions of quartz can be seen in the Si-mapping as lighter spots. New smaller cracks under an angle of 45 degrees have been created and filled later with calcium carbonate, after the fracture has been filled with the green material.

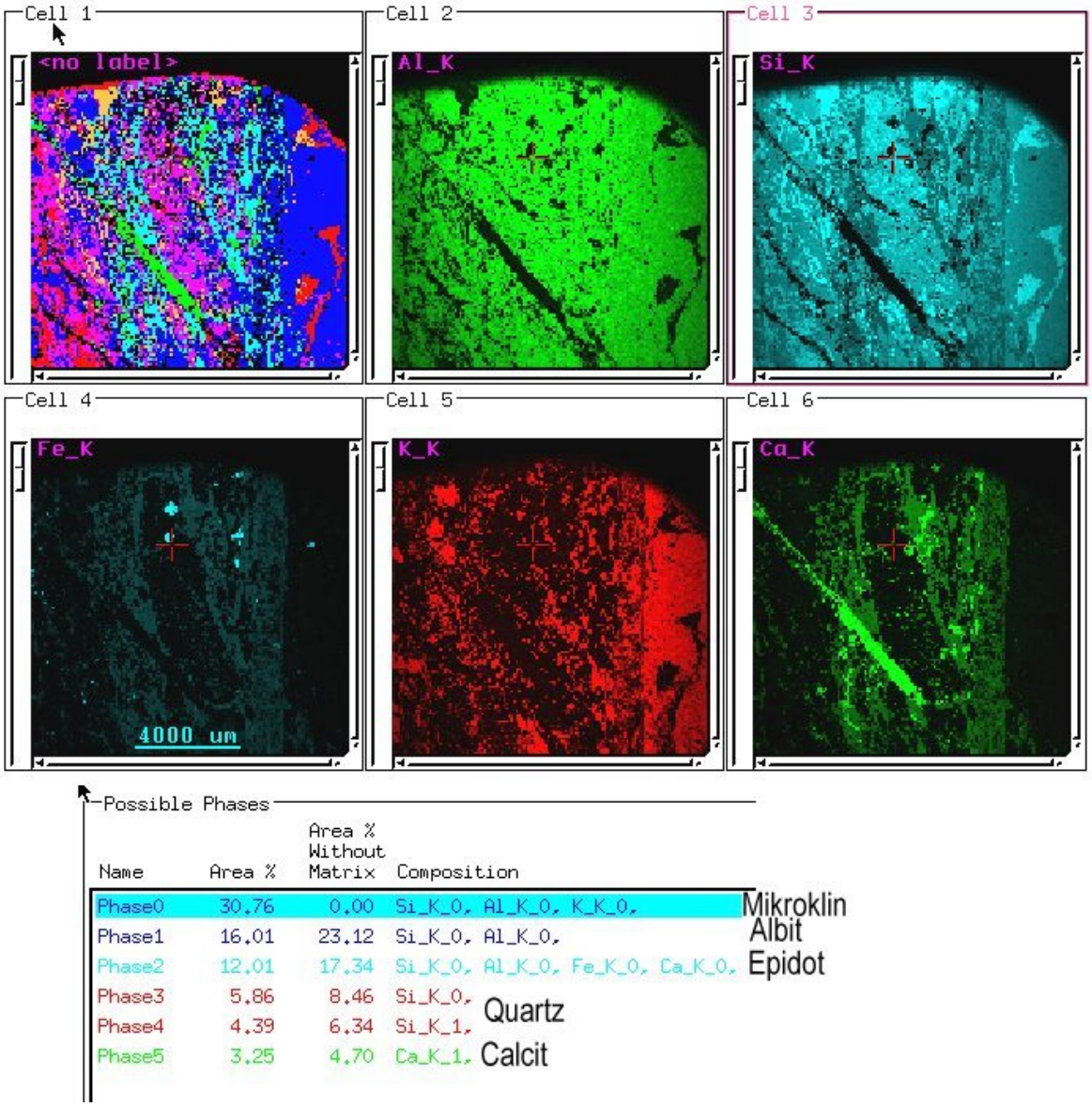

Fig. 17 Element mapping and mineral phases (upper line left) of the fracture

The element mapping images allow to create a mineralogical mapping image. Pixels with the same element content are shown with the same color. Such a picture is integrated in Fig. 17. The minerals selected for the composition are only possible examples, because in this mode no absolute x-ray intensities are calculated from the observed mapping images.

3.3 Determination of the hydraulic properties of the core samples

To determine the hydraulic properties of the core samples, migration experiments were conducted with HTO as the ideal tracer. Fig. 18 shows the breakthrough curves obtained for HTO. The HTO concentration in the eluate was determined by means of an H-3 flow monitor. The pore volumes of the columns were then determined by additional experiments in which the HTO concentration in the eluate was determined by LSC measurements. In this way, the dead volumes to be considered were reduced to a minimum. For column 4, the flow rate was reduced to 0.01 ml/min, as the flow resistance exceeded 50 bar at 0.05 ml/min. The results show that the pore volumes of the fractures in the core samples used were comparable. At a flow rate of 0.001 ml/min, which is an order of magnitude planned for the in situ experiments, it is seen that a higher pore volume is determined because of the matrix diffusion of HTO likely to occur. At the same time, the migration delay results in broadening of the breakthrough curve. The results of the migration experiments, in which the HTO concentration in the eluate was determined by LSC measurement, indicate that the pore volumes of the three fractures examined are approx. 1.0 ml throughout.

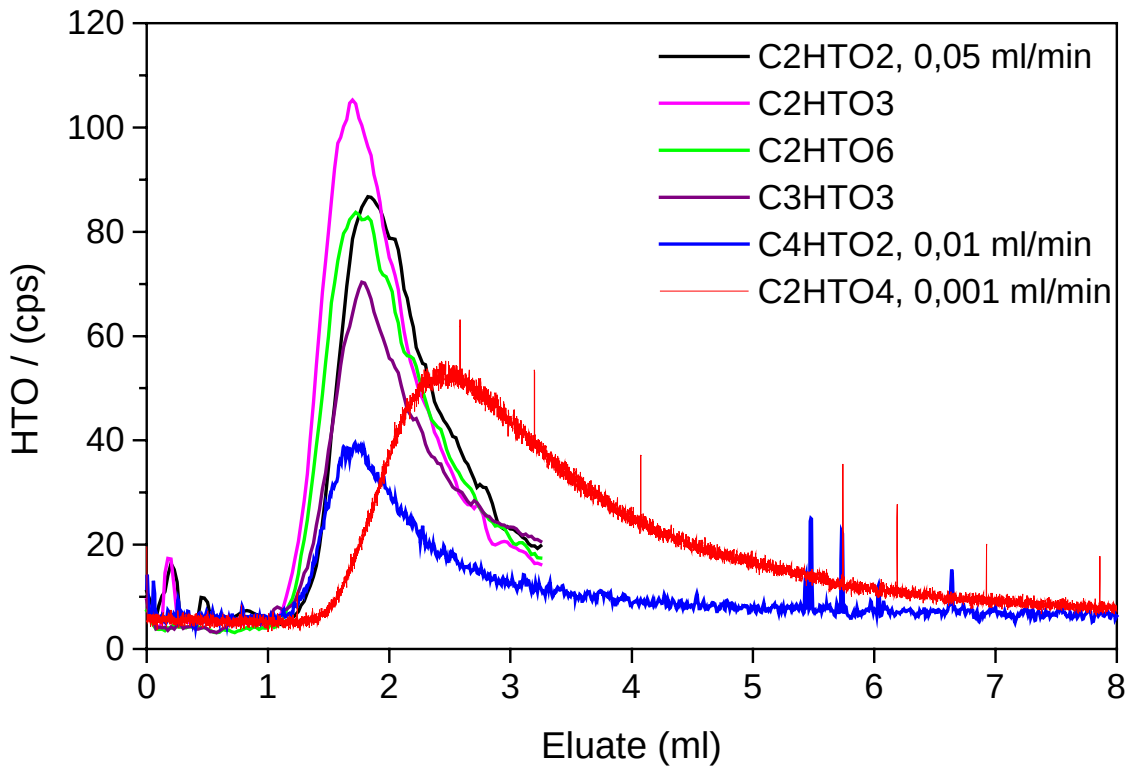

Fig. 18 HTO breakthrough curves for ÄSPÖ columns 2, 3 and 4.

Some characteristic data of the different cores are listed in Table III.

Tab III Characteristic data of the prepared cores

	Core 1	Core 2	Core 3	Core 4
Flow rate [ml/min]	> 0.05	0.05 / 0.001	0.05	0.01
Length	10.5 cm	15.0 cm	18.0 cm	15.0 cm
Pore Volume	~ 0.7 ml	~ 1.0 ml	~1.0 ml	~1.0 ml
Pressure drop	-	12 / 3 bar	23 bar	44 bar
Remarks	Test core	to be used in CHEMLAB	redundancy for CHEMLAB	actinide experiments in laboratory

3.4 HTO Dispersion in the PEEK Line

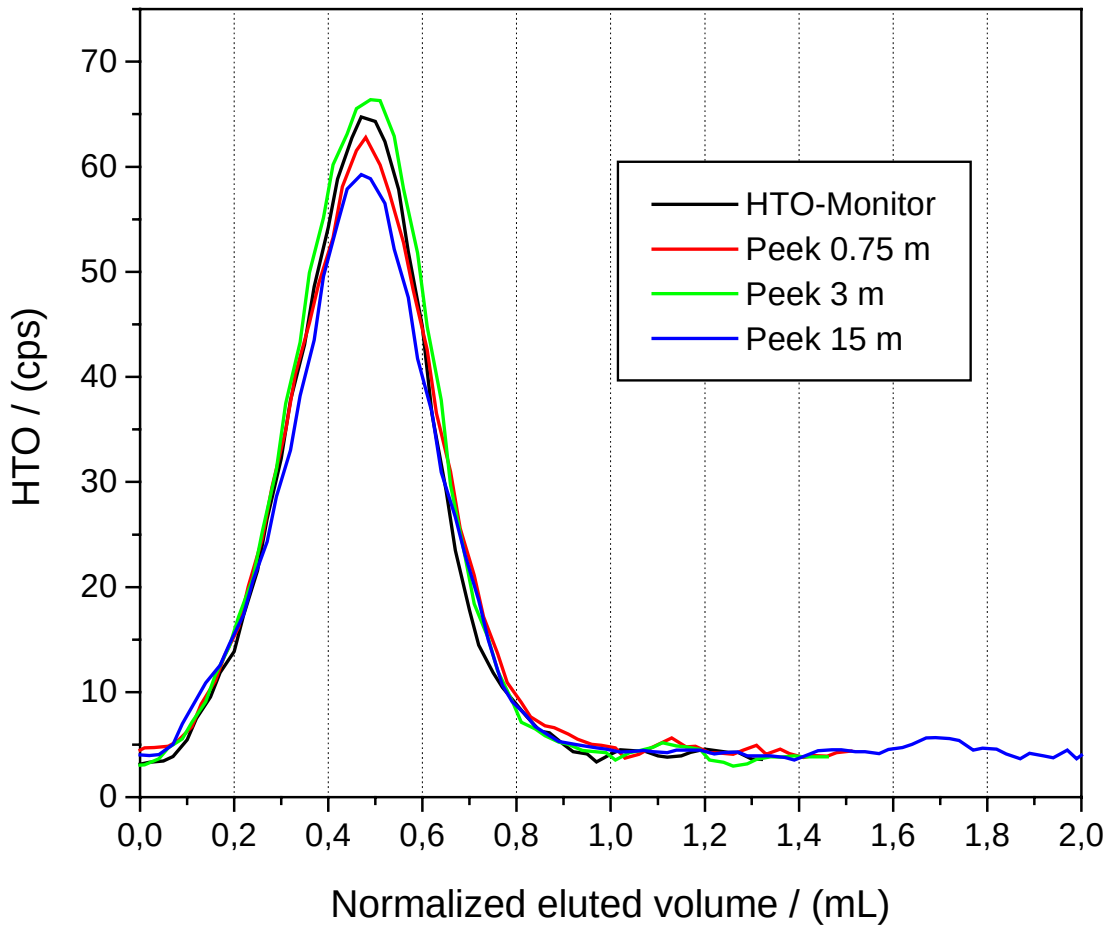

Fig. 19 Effect of the length of a PEEK line on the HTO dispersion (distance between autoclave and sampling station)

In the in situ experiment in CHEMLAB, approx. 20 m of PEEK line is required from the core sample in place to the sampling station in the inert gas glovebox. For this reason, it had to be found out whether the lengths of the line had an influence on dispersion. The measurements of HTO dispersion with PEEK lines of different lengths again were conducted with the HTO flow monitor. Fig. 19 shows the results of the experiments conducted, in which the length of the groundwater discharge line was varied between 0.75 m and 15 m. The results indicate that the length of the PEEK line has no influence on HTO dispersion.

3.5 Laboratory Migration Experiments with a core sample

To prepare the in situ experiments, migration experiments must first be run in the laboratory under largely identical experimental conditions in order to define the experimental boundary conditions for the in situ experiments. This relates particularly to the sampling intervals and to the flow rate.

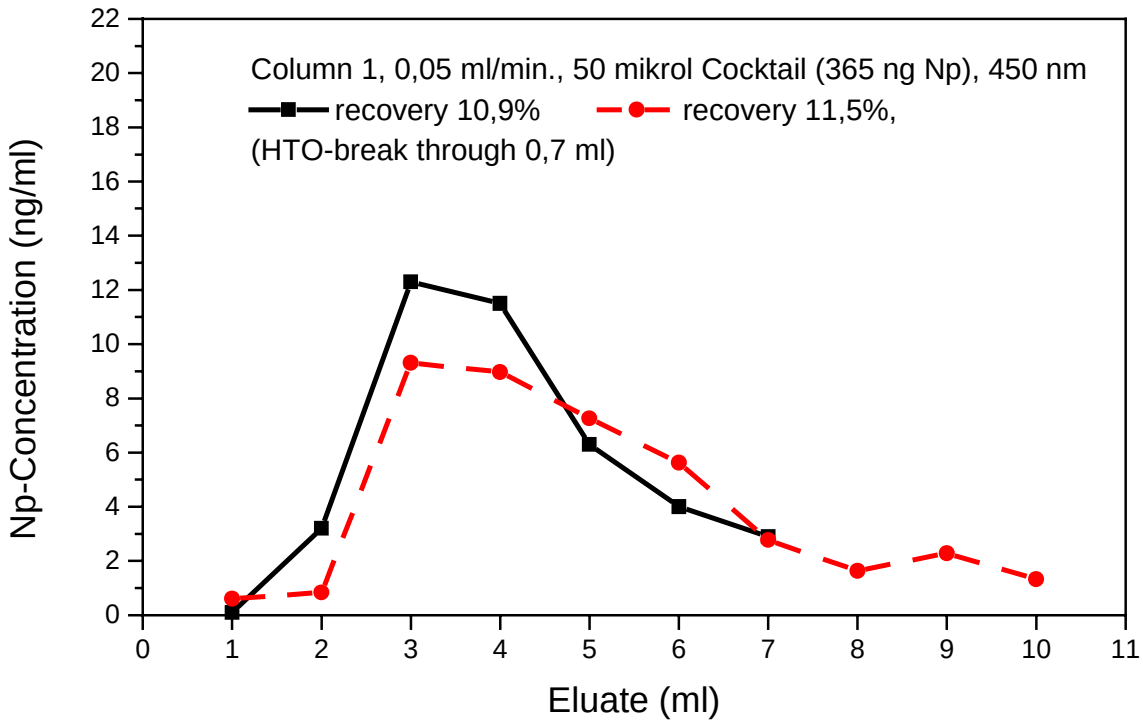

Fig. 20 Breakthrough curve for Np-237 for ÄSPÖ column 1.

Moreover, comparison of the results of the laboratory experiments with the results of in situ experiments is to provide further information about the transferability of laboratory experiments to in situ conditions. For some first tentative experiments, a core sample with a fracture was first employed which was not fit for use in the CHEMLAB-typical laboratory experiments because of its insufficient column length (column 1). The pore volume of this fracture is approx. 0.7 ml. The results of these experiments were to furnish basic knowledge about

the definition of the experimental parameters for the subsequent experiments to be run with core samples typical of CHEMLAB. The migration experiments were run with a so called “ÄSPÖ Cocktail”. This ÄSPÖ cocktail, which was prepared from ÄSPÖ groundwater conditioned with the fracture filling material, contains the three radionuclides to be studied, Pu-244 (1E-8 mol/l), Np-237 (1E-5 mol/l), and Am-243 (1E-6 mol/l). The concentrations of the radionuclides in the cocktail are also listed in Tab X. In these experiments, the radionuclide concentration in the eluate was determined by α-spectroscopy and, at the same time, by ICP-MS measurement. Fig. 20 shows the breakthrough curves obtained for Np-237.

The migration of Np is retarded compared to the migration of HTO; the breakthrough peak occurs at approx. 3 - 4 ml of eluate as compared to 0.7 ml for the HTO breakthrough curve. The recovery for Np-237 is approx. 10%. This result shows that the bulk of Np is retained despite the comparatively short residence time in the fracture. The Np concentration in the eluate does not exceed approx. 4 E-8 mol/l. In some samples of the eluate, also Am-243 was detected in low concentrations in the order of 1 E-11 mol/l. However, because of the low concentrations, these results carry a large error. Moreover, no unequivocal dependence on time of the release of Am-243 can be derived from the values determined.

However, the results show that, even over the relatively short residence time in the fracture, only very small quantities of Am-243 must be considered for migration. This applies also to Pu-244, which was not found in any of the samples examined.

For further preparation of the in situ experiments, laboratory studies are currently being conducted at appropriately lower flow rates on the order of approx. 3 - 5 ml/24 h. Based on the results of the experiments with HTO at the lower flow rate the peak and breakthrough for Np-237 should occur at approx. 5 ml of eluate. Some first results show that no peak concentration has so far been observed up to an eluate volume of 11.0 ml, and that a further reduction of the Np-237 concentration in the eluate is determined on the order of $<$1 E-9 mol/l. These experiments are to be continued to show whether there is a clearly retarded release of Np-237, or whether the release of Np-237 remains clearly lower also over prolonged periods of migration, as a consequence of the increasing influence of the reduction of Np (V) to Np (IV), because of the longer residence time in the fracture.

4 Modelling

4.1 Geochemical Modeling of Actinide Solubilities

The speciation code EQ3/6 was used to calculate the thermodynamic solubility of the actinides Am, Np and Pu. First calculations were performed using one of the standard files, data0.com.V8.R6, as a basis. This file was chosen, because it has the largest number of thermodynamic species available in the concentration range relevant to the **Actinide Migra-**

tion Experiment at Äspö HRL. Consistency checks on the database for the actinides under consideration showed, that it was not possible to reproduce the data of published solubility experiments with the chosen data base. Therefore, all actinide data from the data0.com.V8.R6 file were discarded and replaced with a set of thermodynamic reactions and constants, which was found to describe consistent the published experimental data for actinide solubility. This work was done at INE and is finished for the tri and pentavalent oxidation states. The equilibrium constants used for An(III) and An(V) are taken from literature. (Neck 1998), (Novak 1997), (Neck 1995), (Fanghänel 1995). For the tetra and hexavalent oxidation states a preliminary set of equilibrium constants exists. These constants are listed in the appendix together with their literature references. The notation of the equilibrium constants in this paper is as follows: log β°_{1yz} is 1 metal ion/metal ion unit, y OH^- groups and z CO_3^{2-} groups. For $U(OH)_2(CO_3)_2^{2-}$ the notation is log β°_{122}.

All solubility calculations were performed at 25°C. Solubility calculations were performed for the water composition given in Tab I. $[CO_3^{2-}]$ in the system is controlled up to pH 7.3 by equilibrium with the CO_2 partial pressure of log pCO_2 = -2.5. Above pH 7.3 $[CO_3^{2-}]$ is controlled by equilibrium with $CaCO_3$. In the Fig. 21 to Fig. 24 the relevant pH conditions of the Äspö HRL groundwaters are indicated by an arrow at the pH (x-axis).

Am(III)

Am(III) solubility in Äspö groundwater was calculated to be in the order of 10^{-10} mol/l (Fig. 21). Calculations were performed for different pH values. It was found, that up to pH 7 the Am(III) solubility is dominated by the solubility of $NaAm(CO_3)_2$. From pH 7 to 9 solid $NaAm(CO_3)_2$ is the solubility controlling phase, complexation of Am(III) with OH^- and CO_3^{2-} has to be taken into account. Above pH 9 the solubility controlling phase is $Am(OH)_3$(cr).

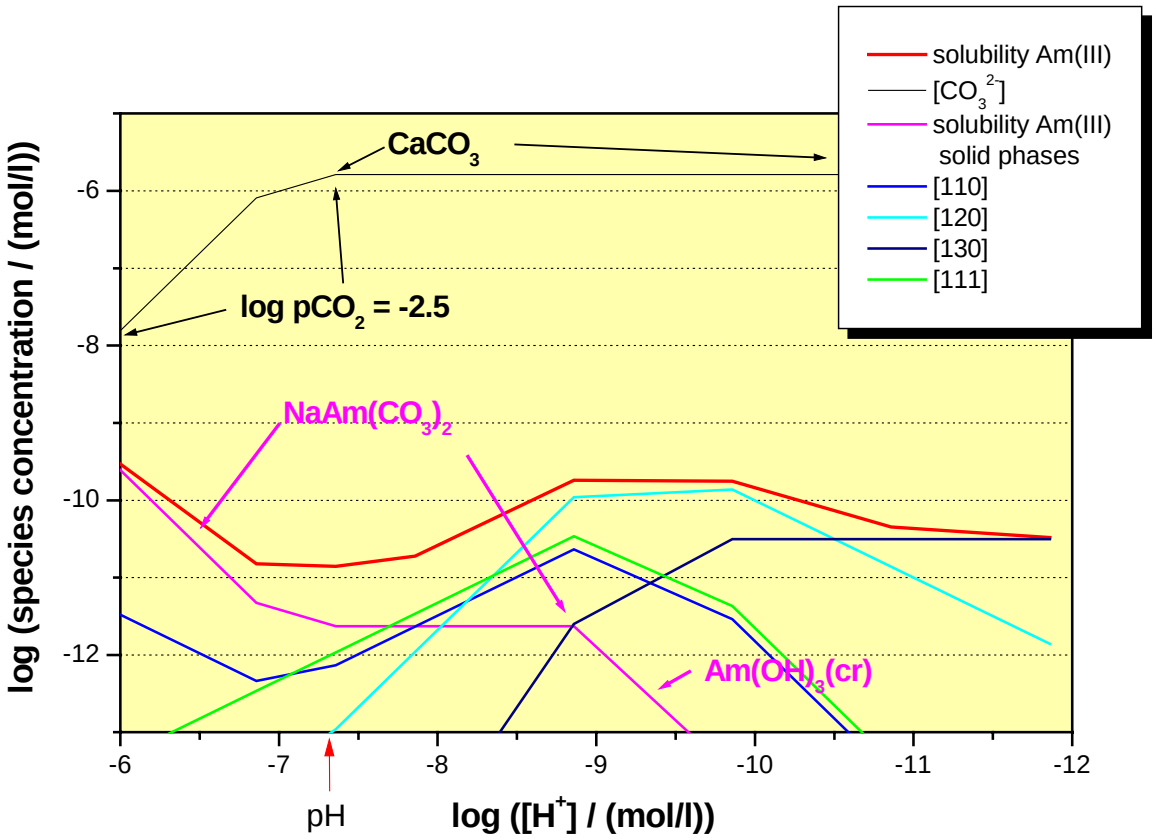

Fig. 21 Am(III) solubility in Äspö groundwatwer

Np(IV/V)

The stable Np oxidation state in the Äspö groundwater is Np(IV) (Eh = -110 mV, pH = 7.5). However, Np(V) is assumed to be meta stable, i.e. Np(V) is transfered by a kinetic hindered redox reaction to Np(IV). For the conditions expected in the CHEMLAB experiment, it is not a priori clear, which redox state has to be expected. Therefore for Np solubility calculations were performed for both redox states. Fig. 22 shows, that Np(V) solubility in Äspö groundwater is rather high and strongly dependent on the pH. For the given pH of 7.5 the solubility was calculated to be about 10^{-3} mol/l. Over the whole pH range (up to pH 12) the Np(V) solubility is dominated by the solubility of Np(V) solid phases. Solution complexation of Np(V) with OH^- and CO_3^{2-} is negligible for the given conditions.

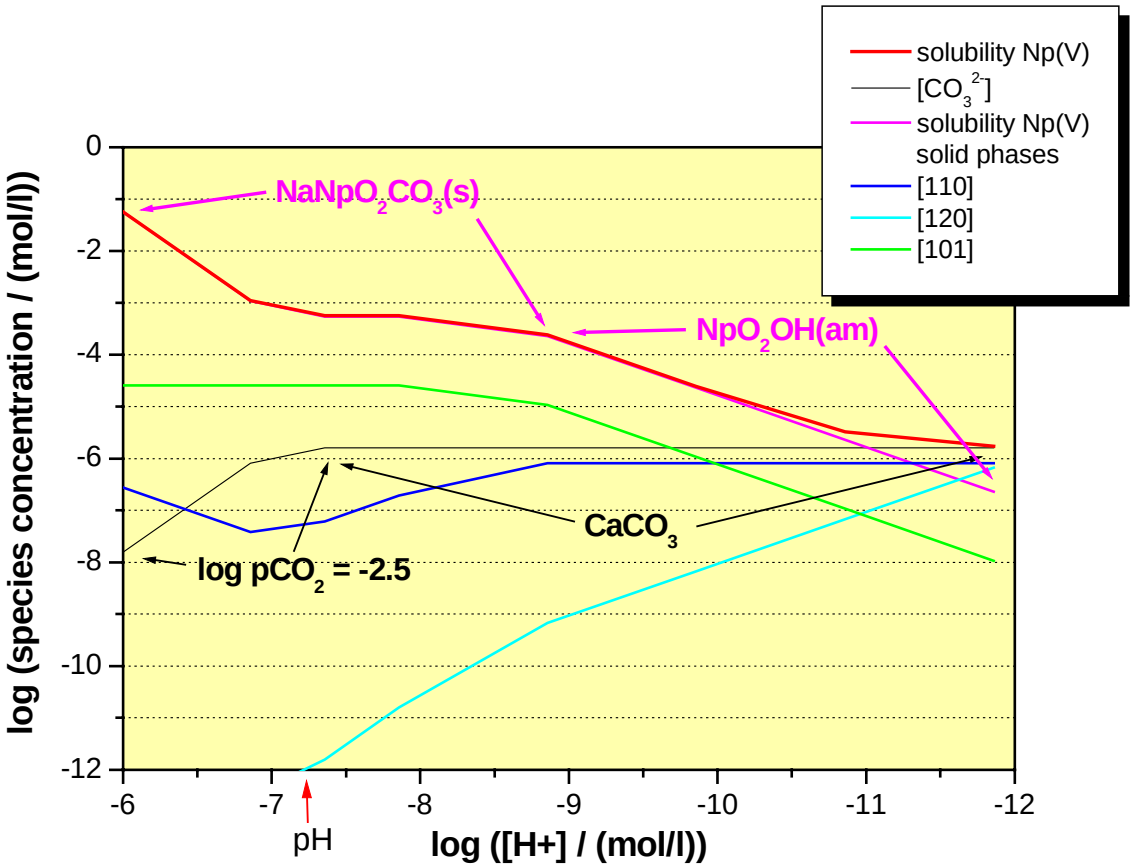

Fig. 22 Np(V) solubility in Äspö groundwatwer

Np(IV) solubility is calculated, too. In this case calculations were performed also for the Grimsel granite groundwater, and a bentonite porewater to be applied in a Grimsel experiment. Only slight changes of the computed Np(V) or the computed Np(IV) solubilities were found for the different groundwaters (Fig. 23). It is evident that the Np solubility depends strongly on the dominating oxidation state: For Np(V) solubilities of 10^{-6} – 10^{-2} mol/l (dependent on pH) were found, whereas Np(IV) solubility is about 10^{-8} mol/l over the whole pH range (6-12) under consideration.

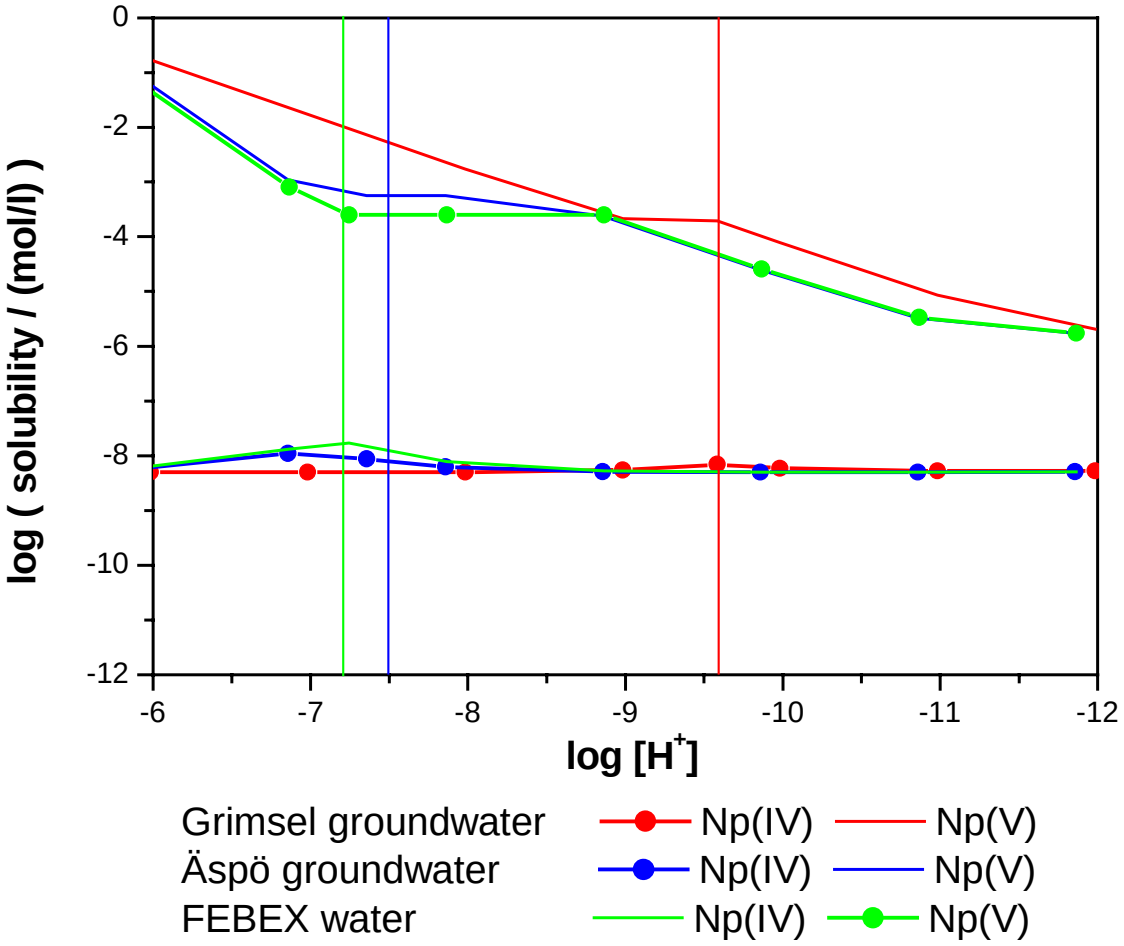

Fig. 23 Comparison of Np solubility at different granite sites: Äspö HRL (Sweden) and Grimsel (Switzerland) having different groundwater conditions

FEBEX: solution in equilibrium with bentonite investigated at Grimsel

Pu(IV)

The tetravalent Pu oxidation state is stable in the Äspö groundwater (Eh = -110 mV, pH = 7.5). Pu solubility calculations were performed only for this oxidation state. Fig. 24 shows, that Pu(IV) solubility in Äspö groundwater is in the order of 10^{-10} -10^{-8} mol/l. Pu(IV) solubility is dominated by the solubility of Pu(IV) hydroxo-carbonato species up to pH 9. Above pH 9 hydrolysis of Pu(IV) becomes more and more dominant.

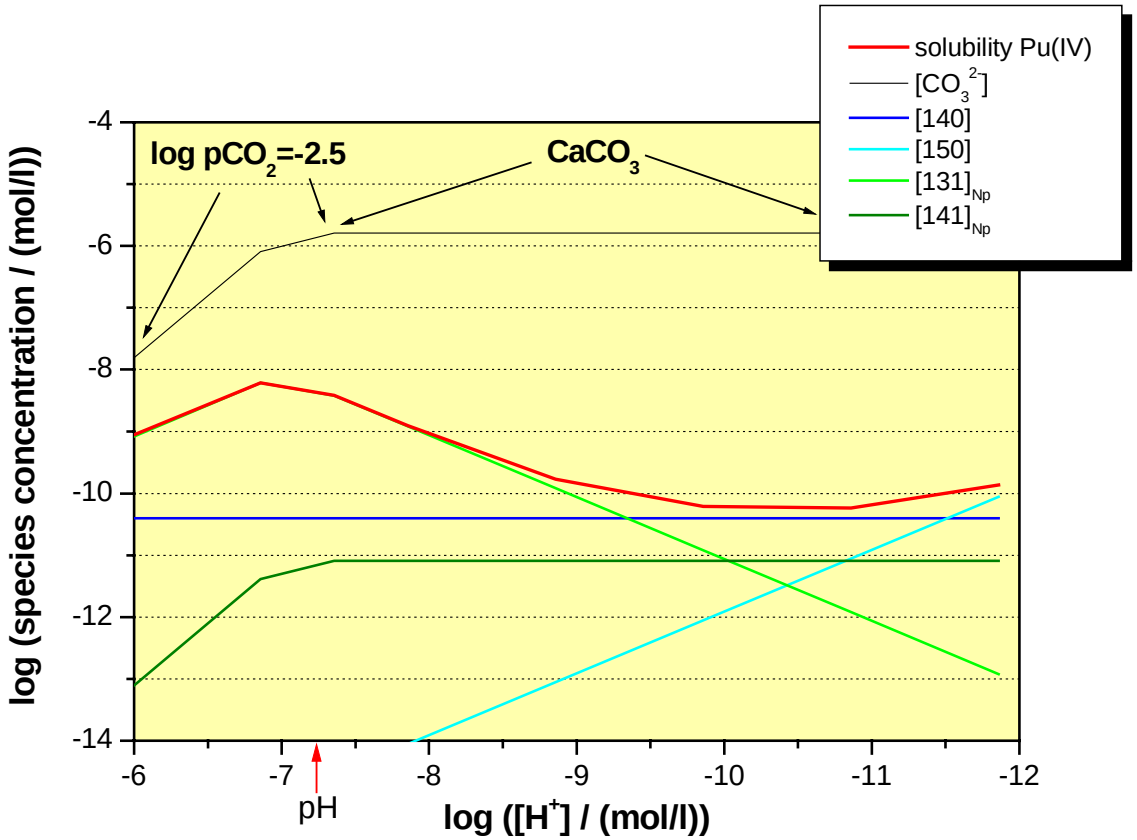

Fig. 24 Pu(IV) solubility in Äspö groundwatwer

4.2 Modelling of tracer tests with column 2 (Hydraulic calibration).

For the two tracer tests performed on column 2 with different flow rates (Test C2HTO2 with 0.05 ml/min and Test C2HTO4 with 0.001 ml/min) first orientating model calculations were performed. As no detailed hydraulic properties of the core sample were known, i.e. porosity and permeability distribution in the fracture and the surrounding rock material, only a crude and tentative modelling was possible so far.

The HTO breakthrough curves are showing marked tails which are typical for the effect of matrix diffusion. Similar shapes of the breakthrough curves, however, could result from more complex conditions concerning the fluid flow and the advective and diffusive mass transport through the sample. The calculations performed up to now were based on the assumption of 1-dimensional flow and transport with matrix diffusion. A special version of the coupled code TRANSAL (fluid flow and mass transport with chemical equilibrium), extended for dealing with matrix diffusion, was used.

As a first step, a separate modelling of the two tests was performed considering a single water conducting zone between two equal porous rock zones. It was found that a satisfactory description of the test results require a quite different choice for the depth and porosity of the porous rock zones for each test. Therefore, a combined model with two successive porous zones on each side of the water conducting zone (Fig. 25) was established, which was found to be capable to give a rather good approximation of the results of both tests (Figs. 2 and 3) with the parameter values given in Tab IV.

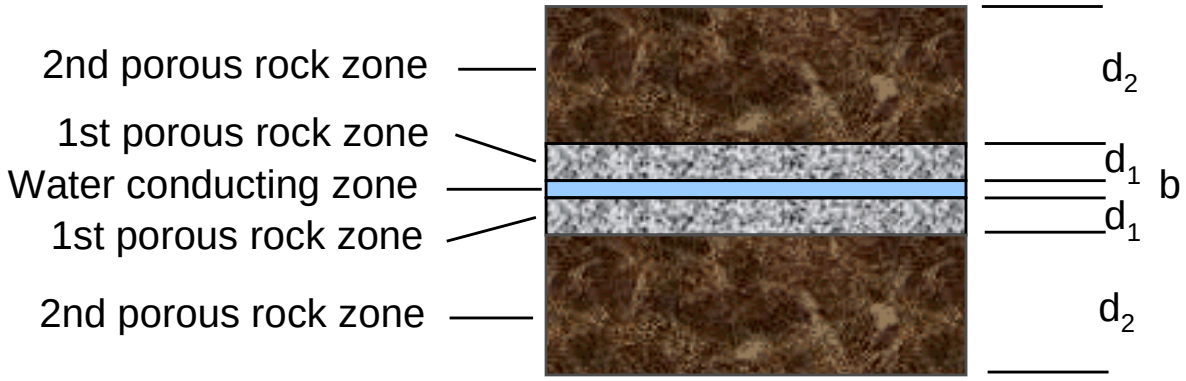

Fig. 25 Conceptual design of the combined matrix diffusion model

Tab IV Parameter values for the combined matrix diffusion model
(letters b, d_1 see Fig. 25)

Water conducting zone	1) b Porosity 2) b Porosity	1.0e-4 / 1.3e-4 m - 1.0e-3 / 1.3e-3 m 0.10
1st porous rock zone	d_1 Porosity	7.0e-4 m 0.056
2nd porous rock zone	d_1 Porosity	4.5e-3 m 0.018

An average diffusion coefficient of 1.e-10 m2/s was used in both porous rock zones.

A longitudinal dispersion length of 0.01 m in the water conducting zone was used. Various definitions are possible for this zone, all of them leading to the same results. Two of them are given in Table IV.

- The first one supposes that there exists a narrow channel without infill within the fracture (of about 1 mm width), and the fracture filling material would represent the porous rock zone 1.

- The second one assumes that the fracture itself with its porous infill represents the water conducting zone, such that the porous rock zone 1 is to be interpreted as a distorted section of the granite core.

In each case, two different values of the parameter b had to be used for the reproduction of the peak delay of the two tests, the larger one for Test C2HTO4 with 0.001 ml/min. This means that here the effective open volume of the flowpath appears to be larger (see also Fig. 18 of Chapter 3.3). The reason for this is not yet understood. A real change of the open volume from one test to the other is not very likely. More complex 2-dimensional distributions of flow and tracer transport, differing significantly for the very different flow rates, may be an explanation.

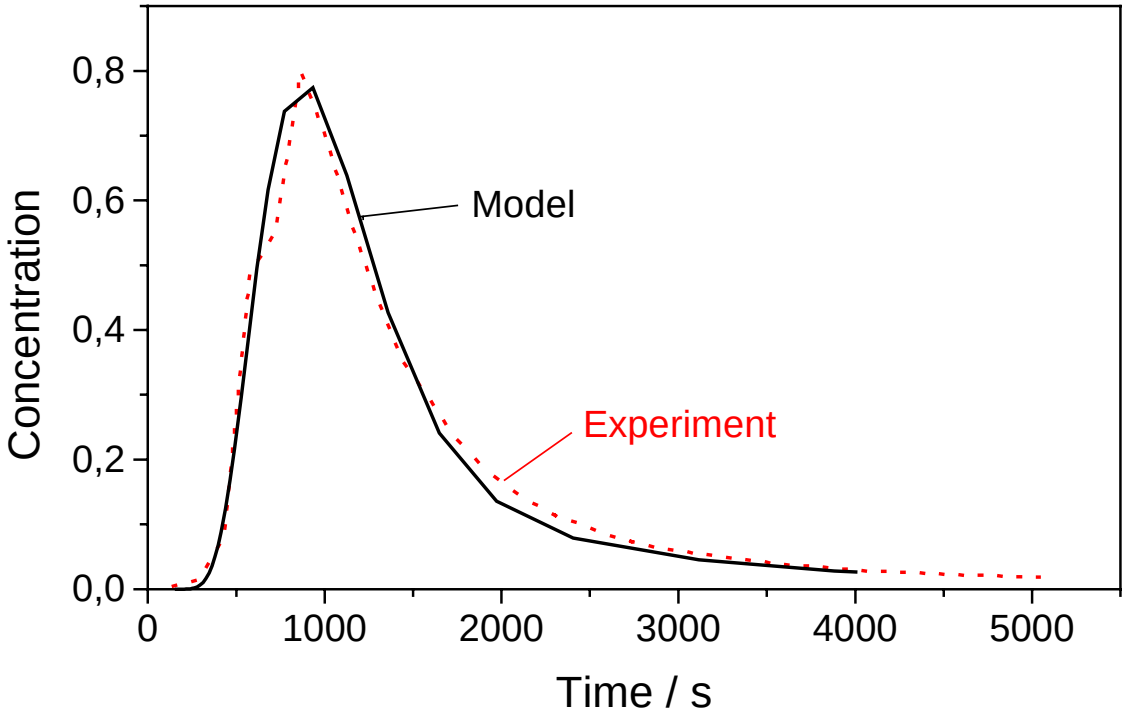

Fig. 26 HTO breakthrough curve of Test C2HTO2 compared to model calculation

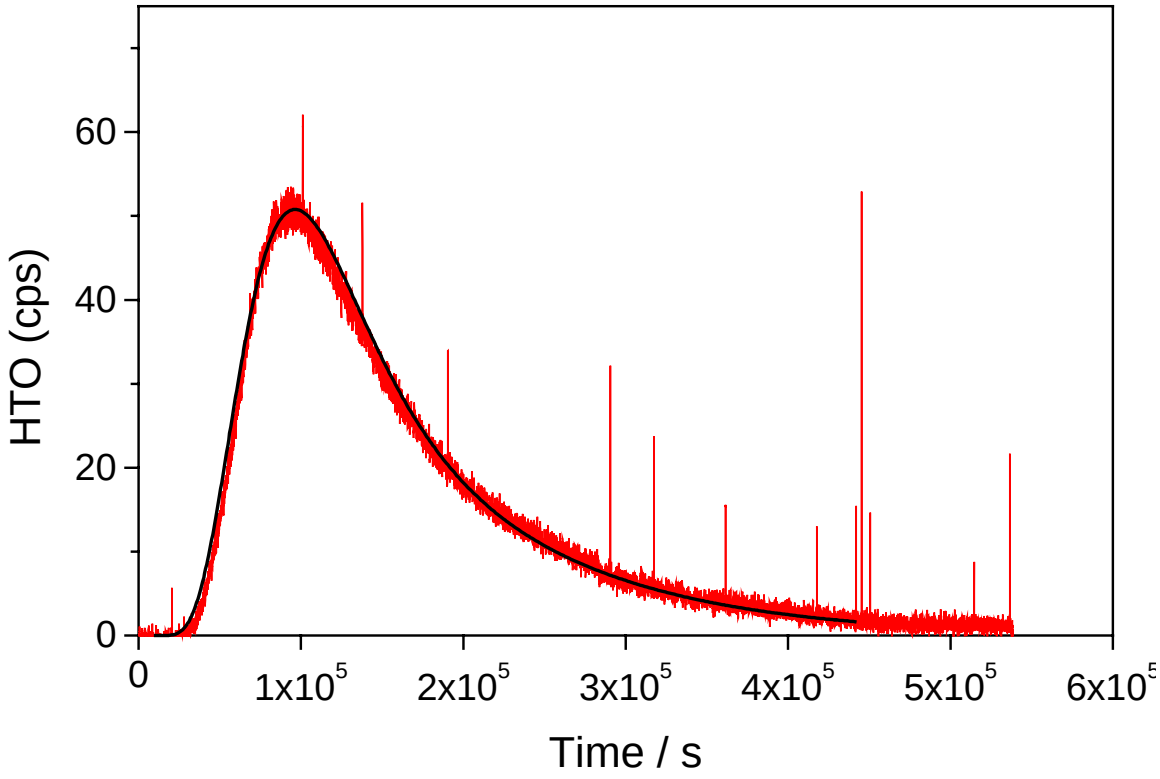

Fig. 27 HTO breakthrough curve of Test C2HTO4 compared to model calculation

In order to obtain a better understanding of the hydraulic and mass transport conditions in these tests, future work will consist in more detailed 2-dimensional model calculations. A final evaluation, however, will be possible only when more detailed experimental investigations of the sample have been performed.

5 Summary

The aim of the work is to investigate the migration and sorption behaviour of actinide elements. Simulation of the complex chemical behaviour, especially the sorption processes, cannot be simulated by other elements. For this reason the most abundant actinides (except U) in spent fuel were selected.

- Am is a representative for the trivalent actinides. It shows a strong tendency to form hydroxo or carbonato complexes at relevant pH. This feature may influence the sorption behaviour. Am may be also sorbed onto inorganic colloids present in the ground water.
- Np can exist in tetravalent or pentavalent state. It is expected from sorption experiments that tetravalent Np species are sorbed strongly whereas the pentavalent state will migrate unretarded. However, under the conditions of the granite (such as the Fe(II) content of the rock) Np(V) will be reduced to Np(IV). It could be shown in batch experiments that this process is subjected to distinct kinetics. The aim of our experiment is to discriminate between the two different valence states and to investigate the different migration/sorption properties.
- Pu shows the most complex chemical behaviour. Especially in the tetravalent state it has a strong tendency to form colloids or to be sorbed onto colloids present in the groundwater. The aim of Actinide Migration Experiment is to investigate how and if Pu migrates under the conditions of Äspö.

Laboratory experiments were run in preparation of in situ migration experiments with Pu, Am, and Np in the CHEMLAB underground laboratory (ÄSPÖ, Sweden).

Batch experiments with the Pu, Am, and Np radionuclides in systems consisting of ÄSPÖ groundwater and fracture filling material, and with ÄSPÖ granite, respectively, show that the radionuclides in the systems are sorbed up to the limit of detection even after relatively short contact periods. Np in this case shows a clear dependence on time, which is attributed to the reduction of Np (V) to Np (IV). Column experiments with Np, which were conducted with only a small column because of the relatively small amount of fracture filling material available, show that, under these experimental conditions, the Np (V) fed is not yet reduced to Np (IV). This would require longer dwell times in the column.

On the basis of the laboratory experiments and the geochemical calculations the conditions for the CHEMLAB experiment could be fixed:

For analytical reasons a rather high chemical concentration of the actinide elements should be applied, in order to have sufficient high concentration in the effluent or on the inner surfaces of our rock sample. Measurements will be performed by means of ICP-MS and not by radioactivity counting. For this reason actinide isotopes could be selected having very long half-lifes and consequently low specific radioactivity. The total activity could be reduced to be in the range of several kBq present in the reservoir of the CHEMLAB:

1.8 kBq Am-243 (containing by 4.1 kBq Cm 243/244)
6.2 kBq Np-237
0.16 Bq Pu-244 (containing 4.3 Bq Pu-239/240)
2.7 Bq Pu-236
0.3 Bq Pu-242

First transport calculations for the HTO tests were performed in order to fit the hydraulic parameters of a fractured rock core. A one-dimensional code was applied considering matrix diffusion. The results however are not unambiguous. From the experiments using different flow rates one can assume that either a narrow channel without infill represents the flowpath

surrounded by porous material (porous rock), or the fracture itself with its porous infill represents the water conducting zone. In the last case, the porous rock zone can be interpreted as a distorted section of the granite core. A final evaluation of the hydraulic and mass transport conditions in these tests, however, will be possible only when detailed investigations of the flowpath have been performed.

6 References

(Jansson 1997) Mats Jansson, Trygve E. Erikson,
CHEMLAB-In-Situ Diffusion Experiments Using Radioactive Tracers, Migration 97.

(Lieser 1991) Lieser K.H., Mühlenweg
Neptunium in the Hydrosphere and the Geosphere, Radiochimica Acta, 43, 27 (1991).

(Eliason 1993) Thomas Eliason
Mineralogy, Geochemistry and Petrophysics of Red Coloured Granite Adjacent to Fractures, SKB 93-06, March 1993.

(Neck 1998) Neck, V.; Fanghänel, Th.; Kim, J.I.
Aquatische Chemie und thermodynamische Modellierung von trivalenten Actiniden;Report FZKA 6110, 1998

(Novak 1997) Novak et al., 1997, J. Solution Chem. 26, 681;

(Neck 1995) Neck et al., 1995, Radiochim. Acta 69, 39;

(Fanghänel 1995) Fanghänel et al., 1995, Radiochim. Acta 69, 169

7 Annex

Tab V: Dependence on time of the radionuclide concentrations (mol/l) in the unconditioned “groundwater + fracture filling material” system

Exp. duration (days)	Am Stock sol. II	Am Sorption s.	Np. Stock sol. II	Np Sorption s.	Pu Stock sol. II	Pu Sorption s.
0	6.35E-09	6.70E-10	3.02E-05	2.35E-05	1.73E-09	1.60E-10
3	5.69E-09	9.28E-11	3.16E-05	2.20E-05	8.00E-10	6.11E-11
8	5.64E-09	5.48E-11	3.35E-05	2.12E-05	5.09E-10	8.93E-12
16	4.44E-09	3.05E-11	3.31E-05	1.36E-05	3.61E-10	4.09E-12
23	2.21E-09	2.53E-11	2.94E-05	4.36E-06	2.68E-10	4.27E-12
37	2.09E-09	2.69E-11	2.58E-05	1.60E-07	2.25E-10	2.53E-12
57	4.17E-09	1.44E-11	2.60E-05	2.76E-08	2.27E-10	1.76E-12
112	2.10E-09	9.94E-12	2.50E-05	3.44E-08	1.97E-10	1.70E-12

Tab VI: Dependence on time of the Am concentration (mol/l) in the conditioned “groundwater + fracture filling material” system

Exp. duration (days)	Stock sol. II <1 mm	Sorption s. <1 mm	Stock sol. II >1 mm	Sorption s. >1 mm
0	3.28E-09	1.77E-10	1.89E-09	5.41E-10
2	1.21E-09	5.79E-11	1.64E-09	1.63E-10
8	3.29E-09	4.66E-11	1.56E-09	8.90E-11
18	1.67E-09	2.09E-11	-	5.24E-11
28	1.52E-09	1.70E-11	1.31E-09	3.56E-11
63	2.20E-09	1.03E-11	2.24E-09	2.05E-11

Tab VII: Dependence on time of the Np concentration (mol/l) in the conditioned "groundwater + fracture filling material" system

Exp. duration (days)	Stock sol. II <1 mm	Sorption s. <1 mm	Stock sol. II >1 mm	Sorption s. >1 mm
0	5.41E-06	2.82E-06	4.79E-06	3.22E-06
2	5.50E-06	2.41E-06	4.69E-06	2.37E-06
8		1.50E-06	5.17E-06	2.11E-06
18		9.27E-07	4.39E-06	1.10E-07
28	4.39E-06	4.33E-07	4.60E-06	3.48E-08
63		9.03E-08	3.53E-06	2.76E-08

Tab VIII: Dependence on time of the Pu concentration (mol/l) in the conditioned "groundwater + fracture filling material" system

Exp. duration (days)	Stock sol. II <1 mm	Sorption s. <1 mm	Stock sol. II >1 mm	Sorption s. >1 mm
0	6.46E-09	7.82E-10	6.46E-09	5.89E-09
2	6.47E-09	3.64E-11	5.39E-09	2.73E-09
8	3.27E-09	1.03E-11	7.16E-10	2.99E-11
18	2.98E-09	4.11E-12	1.28E-10	2.23E-11
28	4.40E-09	5.31E-12	1.42E-10	3.77E-11
63	2.79E-09	3.09E-12	2.01E-09	2.46E-11

Tab IX: Dependence on time of the radionuclide concentration (mol/l) in the "groundwater + fracture backfill material" system

Exp. duration (days)	Am stock sol. II	Am sorption s.	Np. stock sol. II	Np sorption s.	Pu stock sol. II	Pu sorption s.
0	1.04E-09		6.34E-06		8.47E-09	
1	4.49E-10	4.27E-11	6.49E-06	2.03E-06	8.73E-09	1.66E-10
8	4.11E-10	3.74E-11	5.51E-06	4.76E-07	8.17E-09	3.70E-11
18	4.13E-10	1.28E-11	4.42E-06	1.66E-07	6.83E-09	3.18E-11
34	4.12E-10	1.04E-11	4.18E-06	6.62E-08	2.54E-09	1.30E-11

Tab X: Radionuclide concentrations in the ÄSPÖ cocktail

Pu-244	approx. 1 E-8 mol/l
Am-243	approx. 1 E-6 mol/l (in situ 1 E-8 mol/l)
Np-237	*approx. 1 E-5 mol/l*

(Dilution and measurement with ICP-MS indicated that concentrations of up to approx. 1 E-12 mol/l can be measured with sufficient accuracy.)